

LOW TEMPERATURE ULTRAMICROINCINERATION OF THIN-SECTIONED TISSUE

WAYNE HOHMAN and HARALD SCHRAER

From the Department of Biophysics, The Pennsylvania State University, University Park, Pennsylvania 16802. Dr. Hohman's present address is the Department of Obstetrics and Gynecology, Section of Experimental Pathology, Women's Hospital, Los Angeles County—University of Southern California Medical Center, Los Angeles, California 90033.

ABSTRACT

Low temperature ultramicroincineration was employed to determine the morphological localization of "structure-bound" mineral and/or metallic elements within biological cells at the electron microscope level. This technique chemically removes organic material from thin sections of tissues with reactive, excited oxygen instead of heat as used in a furnace. The remaining ash representing the mineral/metallic ultrastructure of cells is advantageous for ultrastructural studies because incineration without applying heat is less destructive than the burning associated with high temperatures. This low temperature incineration method was applied to thin-sectioned avian shell gland mucosa, a calcium transporting system, as a sample tissue. The results include: recognition of many subcellular organelles in the ash patterns, identification of dense, ash-containing granules (possibly organic-metallic complexes) in epithelial cells which may be involved in calcium transport, description of ashed erythrocytes and collagen, comparison of ashed glutaraldehyde fixed tissue with and without osmium postfixation, description of lead-stained cells after ashing, demonstration that ash preservation is dependent upon section thickness, illustration of the fine resolution obtainable because the ash residues remain relatively near their *in situ* origins, discussion of technical problems in this relatively new field, and demonstration of the presence of Ca and P in the ash with electron microprobe X-ray analysis.

INTRODUCTION

Visualization of metallic substances within cells can be accomplished with low temperature ultramicroincineration—the technique of chemical incineration at the electron microscope level. Low temperature incineration selectively removes organic matter from specimens with a stream of very reactive, excited oxygen. Metallic and/or mineral substances remain near their *in situ* positions with good preservation of spatial integrity. Due to the specimen preparation methods such as fixation, dehydration, and sectioning which employ aqueous solutions, the ash observed after low temperature incineration is the insoluble or

"structure-bound" mineral (Renaud, 1959; Boothroyd, 1964, 1968; Thomas, 1964, 1969). Low temperature incineration is an improved approach to classical high temperature incineration.

In this study, low temperature ashing was applied to thin sections of the avian shell gland as an example utilizing this technique. The use of avian shell gland arose from interest in the cellular process of calcium translocation in this specialized calcium transport system (Schraer and Schraer, 1965, 1970, 1971; Hohman and Schraer, 1966). This tissue is a natural model for the study of calcium transport because it handles the movement

of this metal from blood to ultimate crystallization as CaCO_3 on egg shells. Current knowledge of the structure and function of the avian shell gland in calcium translocation has been reviewed and summarized by Schraer and Schraer (1970). The histology and cytology of this tissue have been described extensively by light microscopy (Surface, 1912; Bradley, 1928; Richardson, 1935; McCallion, 1953) and electron microscopy (Johnston et al., 1963; Breen, 1966; Makita and Nishida, 1966; Breen and De Bruyn, 1969; Nevalainen, 1969).

The history of low temperature microincineration of thin-sectioned biological material (ultramicroincineration) has been brief. Turkevich (1959) had the foresight to suggest that the "(excited oxygen) method of microincineration can be extended to the study of biological tissue sections", adding that incineration before and after staining with electron stains could be useful. Thomas (1962) was the first to show electron microscope ash patterns of ultrathin sections of a biological material, although this initial study employed only high temperatures. Thomas (1964) extended this study to pioneer low temperature incineration of thin-sectioned biological materials for examination in the electron microscope. After his initial study on *Bacillus megaterium* spores, he applied low temperature ashing to thin-sectioned, isolated, calcium phosphate-loaded, mitochondria, (Thomas and Greenawalt, 1964, 1968), *Tipula* iridescent viruses (Thomas, 1965), and plant cells (Thomas, 1967). The techniques of Thomas were used with high temperature ashing to demonstrate the mineral nature of granules in strontium-loaded mitochondria (Greenawalt and Carafoli, 1966). After these demonstrations of the high resolution capabilities of low temperature ashing on sectioned bacteria, viruses, and isolated mitochondria, Hohman and Schraer (1967) and Hohman (1967) initiated their studies with this technique on thin-sectioned shell gland tissue and described the intracellular "mineral ultrastructure" of cells. Subsequently, the intracellular ash content of two other thin-sectioned tissues (rat epididymis and kidney cortex) has been described at the electron microscope level (Boothroyd, 1968); however, only high temperature ashing was employed. Doberenz and Wyckoff (1967) used excited oxygen incineration on ultrathin sections of fossilized teeth. The results from all of these studies on thin-sectioned material have been summarized and discussed in

an excellent review on the current status of spodography (for both high and low temperatures and at both light and electron microscope levels) by Thomas (1969). Subsequent to this review, additional ultramicroincineration studies employing only high temperatures have been used to investigate the mineral nature of dense granules in thin-sectioned rat bone and intestine (Martin and Matthews, 1970; Matthews et al., 1970; Sampson et al., 1970). Low temperature ultramicroincineration has not previously been employed to determine the mineral ultrastructure of a tissue.

Since this is the first extensive application of low temperature incineration to thin-sectioned tissue, this work presents an exploratory sampling of what possibilities exist employing this technique. The principal current limitations are (a) the nature and extent of mineral losses during preparation, thereby limiting the results to structure-bound material, and (b) the lack of identification and localization of specific minerals or metals within the tissue cells. The extent of and attempts to overcome these limitations are included in the Experimental Results and Discussion. However, there are also advantages that illustrate the current and potential value of this technique. The advantages are: (a) a relatively unambiguous technique to demonstrate electron opacities which arise from intrinsic mineral loads rather than only from osmium or electron stain affinities, (b) a demonstration of the very detailed resolution obtainable from tissue by ultramicroincineration, (c) an approach that yields information for reasonable speculation on the chemical nature of the ash and its physiological importance (dependent upon the specific system studied), (d) an aid to studies on the general chemical nature of observed structures, whether organic, organic-metallic, or metallic (i.e. electron stains), and (e) a starting point for solving the current limitations. If the identity of specific mineral substances in their *in situ* locations within tissue cells becomes possible, this technique would be an invaluable research tool of general interest.

METHODS¹

The techniques for low temperature ultramicroincineration described in this study were patterned after those used by Thomas (1964, 1969²), but were

¹ For more detailed description and discussion of the methods used in this study, refer to Hohman (1967).

² Through the courtesy of Dr. Richard S. Thomas, the authors had access to a prepublication version of this reference in 1966.

developed uniquely for this study. Boothroyd (1968) also used and described similar preparative techniques for his high temperature work. These references are the principal sources for biological ultramicroincineration methodology.

Grids

Punched 200 mesh, molybdenum grids which were notched with a razor blade to provide a reference point in the electron microscope were used in this study. The essential requirement for the grids is that they do not react with the excited oxygen. Copper grids do react and are not suitable for low temperature ashing. It is preferable that the grid holes be relatively small and flat to provide sufficient contact area for the silicon monoxide support films. Woven wire, stainless steel grids and titanium grids with large, oblong holes were eliminated because both have less accessible surface area.

Silicon Monoxide Support Films

The support film for the low temperature ashing must be inorganic to prevent reaction with the excited oxygen, be composed of low atomic number elements to be electron-transparent, be stable to withstand heat generated by the electron beam, be amorphous to prevent limiting electron microscope resolution, be sufficiently strong to survive high vacuums and handling, be water insoluble to prevent dissolution during section mounting and staining, and have a reasonably low vaporization point for ease of preparation. Silicon monoxide (SiO) meets these requirements (Williams, 1952; Hass and Meryman, 1954; Kafig, 1958; Thomas, 1964, 1969; Boothroyd, 1968).

The SiO support films were prepared as follows. Formvar was cast on glass according to a slightly modified method of Drummond (1950). The Formvar-coated slides were mounted in a vacuum evaporator about 10 cm above a tungsten boat (made from 1 mil, 1.25 inch \times 0.25 inch tungsten ribbon) which contained 6 mg (an excess quantity) of degassed (see Hass and Meryman, 1954), powdered SiO. The SiO was evaporated for 5 min at 25 amp filament current in a vacuum of about 4×10^{-4} torr.

The evaporation amperage was determined experimentally to yield a near minimal temperature required for SiO evaporation (see Hass and Meryman, 1954, for a discussion of the chemical nature and purity of evaporated SiO films). Evaporation at higher temperatures resulted in the formation of electron-scattering residues after contact with water (Williams, 1952). The evaporation time was obtained by experimentally determining a satisfactory thickness for the SiO layer. This thickness was estimated by observing the interference colors (Hass

and Meryman, 1954; Kafig, 1958) depicted on a small piece of front-surfaced mirror (heavy chromium layer on a glass slide). A light yellow or gold color was deposited during the 5-min evaporation time.

The SiO-Formvar combined films were transferred from the slides to the grids according to the "ring tool and peg" method (Drummond, 1950). The films had silver reflections in fluorescent light while floating on water. After drying on the grids, most of the films appeared relatively smooth under a low magnification microscope. The Formvar layer lying on top of the SiO layer was removed in the low temperature asher (LTA) which was operated at the same levels used for specimen incineration. This final step caused a noticeable change in the smooth, relatively flat appearance of the films as though the films expanded and sagged. This was unavoidable, but it produced no serious disadvantages except for local variations in the shadowing angles. The method yielded SiO support films attached directly to the grids with no intermediate or interfering layers.

It was important to control carefully the thickness of the SiO films. SiO films alone were very brittle and shattered readily during preparation; on the other hand, Formvar films alone were flexible and handled easily. The handling of SiO-Formvar combinations ranged progressively between these two extremes as the SiO thickness was increased. By using the pale yellow interference color to determine the SiO thickness, films used in this study were estimated to be less than 500 Å (Hass and Meryman, 1954; Kafig, 1958). Shadowed fragments of the film used by Thomas (1969) indicated that his support films were about 175–350 Å thick.

Fixatives

BUFFER: *S*-collidine (2,4,6 trimethylpyridine) was selected as an organic buffer to avoid introduction of metallic elements in the fixative solutions (Bennett and Luft, 1959). A 0.1 M *s*-collidine stock solution was prepared in glass double-distilled water and adjusted to pH 7.2 with pure acetic acid (approximately 3.5 ml/l). Note that an organic acid was substituted for HCl which normally is used with this buffer. In addition to presumably volatilizing in the LTA, *s*-collidine is an exceptionally good buffering agent in the pH range used.

OSMOLALITY: Osmotic conditions during fixation were adjusted cryoscopically to approximately 296 mosmols, the osmolality of hen plasma (Korr, 1939). This osmolality was selected as the most reasonable choice available since the intracellular tonicity was unknown.

COMPOSITION: Glutaraldehyde was selected as a fixative that contained no inorganic atoms. A 1.25% (0.133 M) glutaraldehyde (Fischer, biological grade, 50%) solution in the 0.1 M *s*-collidine-acetic

acid buffer (pH 7.2) was used (Sabatini et al., 1963). The osmolality was 310 mosmols. A 1% (0.04 M) osmium tetroxide solution in 0.1 M *s*-collidine-acetic acid buffer (pH 7.2) was prepared for use as a postfixative and its osmolality adjusted with 0.11 M sucrose. The final osmolality of the osmium fixative was 304 mosmols. A buffered wash was prepared by substituting an equivalent amount of sucrose (0.133 M) for the glutaraldehyde in the fixative. Since glutaraldehyde and sucrose contribute almost equally to the osmolality (Maser et al., 1967), no further adjustment of the osmolality was necessary. The osmolality of this solution was 302 mosmols.

Preparation of Tissue

Mature white Leghorn hens sacrificed by decapitation provided the shell gland tissue which was excised, sampled, and rapidly placed into the glutaraldehyde fixative. All samples were taken from the pouchlike midportion of the shell gland. The tissues were fixed for approximately 2 hr in glutaraldehyde and washed overnight in the buffered wash. A portion of these samples were postfixated in the osmium tetroxide for 2 hr. All tissue samples were dehydrated and embedded in Epon (Luft, 1961). Sections were cut at various thicknesses as noted in the Experimental Results. In an attempt to minimize extraction of soluble minerals, all sections were cut onto 0.001 M ammonium bicarbonate at approximately pH 7.6 (Thomas, 1969). Staining was generally avoided to prevent introduction of extraneous metals. In one experiment, sections were stained with lead citrate (Venable and Coggeshall, 1965) to explore the feasibility of studying stain affinity sites with low temperature ultramicroincineration.

The Low Temperature Asher

The low temperature asher (Tracerlab Div., Richmond, Calif., LTA-600) converts relatively unreactive molecular oxygen to an excited plasma which removes organic substances and leaves mineral deposits (see Gleit and Holland, 1962; Gleit, 1963, 1965, 1966; Hollahan, 1966). The excited plasma is formed as molecular oxygen passes through an electromagnetic field. This plasma is not fully defined, but its partial composition includes atomic oxygen, excited molecular oxygen, ionized forms of oxygen, free electrons, ground-state oxygen molecules, and various forms of impurities and reaction products (for details consult Foner and Hudson, 1956; Herron and Schiff, 1958; Elias et al., 1959; Ogryzlo and Schiff, 1959; Kaufman and Kelso, 1960; Marsh et al., 1963; Gleit et al., 1963; Marsh et al., 1965 a, 1965 b; Bersin, 1965; and Hollahan, 1966). The excited oxygen is substituted for heat as used in classical incineration as the source of energy for the ashing

process. The organic matrix of specimens is removed in a relatively gentle manner because the effects of heat, such as melting, charring, coalescing, fusing, etc. are minimized or eliminated. Since the ash residues are left relatively close to their *in situ* positions, this technique is particularly advantageous for ultramicroincineration studies with the electron microscope. Thomas (1969) has reviewed the development of the low temperature asher and its past uses.

In this study, the grids containing sections were positioned about 2.5 cm from the front edge of glass slides inserted into the glass oxidation chambers of the LTA. The LTA was operated at a low forward power level (50 watts) at minimum reflected power (about 2 watts), 70 cc/min (STP) oxygen flow rate, and about 0.7 mm Hg pressure. Standard incineration time was 20 min which was probably excessive for thin sections. Repeated incineration after 20 min produced no further change in the appearance of the specimens in the electron microscope. At this low power level, the discharge will not "strike" spontaneously nor maintain itself at significantly greater gas flow rates, higher pressures, or untuned power settings. The power level and tuning were preset without a specimen, the gas flow and pressure were adjusted after the specimen was inserted, and the discharge was initiated with a Tesla high frequency induction coil (Tesla Electric Co., Chicago, Ill.) These steps assured constant oxidation rates at minimal operation levels to yield mild ashing conditions.

Postincineration Procedures

PRESERVATION OF THE SIO SUPPORT FILMS: Even with the satisfactory support films prepared as described above, the support film/specimen combinations sometimes were destroyed by the electron beam in the electron microscope after ashing while adjacent areas covered with support film alone were stable. It is possible that the specimens and support films react during ashing (Thomas, 1969). Regardless of the cause, it was eliminated when necessary by evaporating a thin layer of carbon on top and bottom of the grid after ashing but before viewing. To coat the bottom surface, the grids were inverted over holes in a metal frame that supported the grids at their outer circumference.

PRESERVATION OF THE ASH: The ash which resulted from the incineration treatment appeared stable and required no special ash preservation precautions. The ash adhered well to the support films, there was no apparent water absorption, and neither grid inversion, exposure to air and vacuums, shadowing, nor the electron beam noticeably altered the observed ash patterns.

SHADOWING: Although the contrast of ashed samples in the electron microscope was adequate

without shadowing, some samples were shadowed with platinum (Bradley, 1965) to enhance the contrast and demonstrate three-dimensional shapes.

MAPPING: To relocate specific areas in the electron microscope after incineration and other treatments, the locations of the sections on grids were mapped in reference to the notched marker by using a stereomicroscope. For orientation, surveys of grids began at the tip of the notched markers. Specimens were viewed, treated, and previewed as many times as desired (see Boothroyd, 1968).

ELECTRON MICROPROBE ANALYSIS: An electron microprobe was used in preliminary trials to study the feasibility of identifying the ash components. Ashed samples of several thicknesses from various preparations were observed in the electron microscope and then transferred to the electron microprobe for analysis by scanning areas and/or traversing a small, focused spot. After specimens were traversed with a small spot, the pathways of the traces were visible in the electron microscope. This made it possible to coordinate the numerical and graphic output data with the actual path the electron beam had followed on the specimen. Some results will be presented and discussed to indicate possible applications based on these preliminary trials.

EXPERIMENTAL RESULTS

Shell Gland Mucosal Cells

The shell gland mucosa consists of a columnar epithelium which lines the central shell gland lumen where the calcium deposition occurs and tubular glands which lie below the columnar epithelium.

EPITHELIAL CELLS: Low magnification electron micrographs of conventionally fixed (glutaraldehyde with osmium postfixation) and stained lead citrate and uranyl acetate thin sections of the epithelial cell layer are shown in Figs. 1 and 2. The columnar epithelium consists of two main cell types—ciliated, apical cells (A) and nonciliated, basal cells (B). Both cell types are lined with microvilli (mv). Goblet cells, a third type of cell, are relatively few in number and none are included in these electron micrographs. The apical and basal cells are named and distinguished by the characteristic luminal and basal locations of their nuclei (see Figs. 3 and 4). The membranes surrounding the nuclei are distinct and there are dense areas (nucleoli) within the nuclei. Especially prominent in these micrographs are spherical, black granules. Although the granules are scattered throughout both apical and basal cells as seen in Figs. 1 and 2, they are commonly concentrated in clusters near

the lumen (L) in both apical and basal cells and on the luminal side of nuclei in basal cells only. The granules in basal cells (g_1 in Figs. 1 and 2) usually appear small, dense, and round. The granules in the apical cells (g_2) are often larger and membrane-bounded (see Nevalainen, 1969). Elsewhere in the cytoplasm, mitochondria, endoplasmic reticulum, and small vacuoles are easily identified. Particularly note that the cell membranes separating adjacent cells are readily discernible.

Sections of shell gland similar to those shown in Figs. 1 and 2 were low temperature incinerated and are shown in Figs. 3 and 4. Fig. 3 is from tissue fixed only in glutaraldehyde, sectioned at approximately 0.5μ , unstained, and incinerated in the LTA. Fig. 4 is similar to Fig. 3 except that in addition the tissue was postfixated in osmium. Fig. 3 had no metallic substances added at any preparative step; Fig. 4 has only osmium added.

In both Figs. 3 and 4, the over-all retention of metallic/mineral substances is substantial. Recognition of the cell types and their location, in this case columnar epithelium, was not only possible but relatively easy. Among all the intracellular components, the apical (a) and basal (b) nuclei are the most prominent features remaining in the ash residues after the low temperature incineration treatment. Most of the nuclei contain irregular, dense regions (some of which are probably nucleoli) within relatively uniform nucleoplasmic ash, features which are seen in conventional micrographs (Fig. 1). The nuclear membrane regions are dense and somewhat irregular. Clear zones or "halos" which are not seen in conventional micrographs (Fig. 1) are observed surrounding the nuclei. In some cases, only a portion of the nuclear periphery shows the clear zones, but generally they are as obvious as in the nucleus (a) of Fig. 3. A dense nuclear border and its adjacent clear zone are shown more distinctly in Fig. 5 which is a detailed view of a glutaraldehyde fixed, incinerated, and platinum shadowed nucleus. The shadows show that the dense ash border possesses significant height. The ash border is approximately 600 Å wide and the clear zone or halo is approximately 2000 Å wide. The dense circular region within the nucleus (nucleolus) is not bordered by a dense band of ash as is the entire nucleus, but it does appear to be surrounded by a clear zone. Fig. 4 shows one nucleus (N_t) that was sectioned in a near tangential plane whereas most of the other nuclei were cross-sections. Unlike the cross-sections

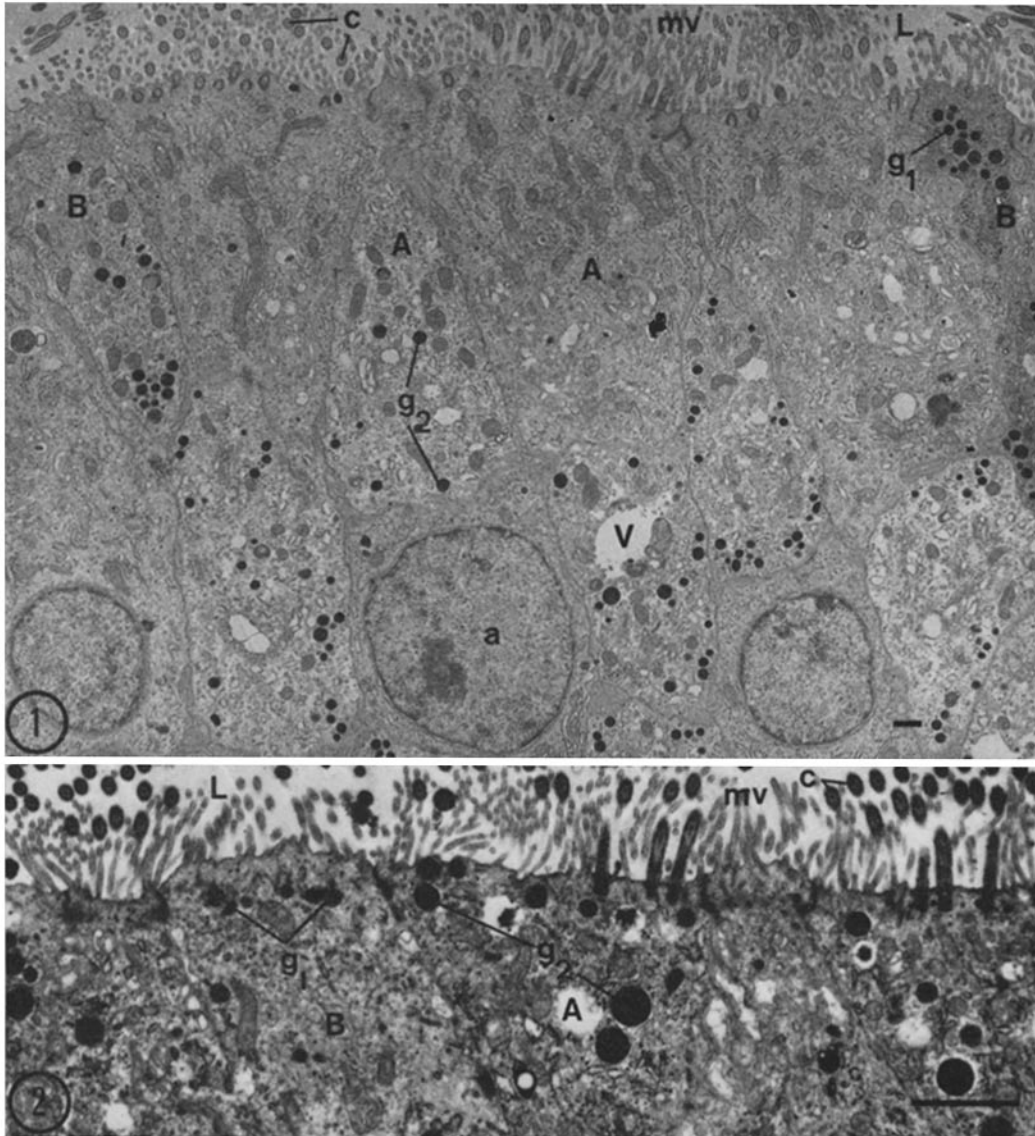


FIGURE 1 Conventionally prepared electron micrograph showing epithelial cells of the shell gland mucosa (glutaraldehyde fixed, osmium postfixed, uranyl acetate and lead citrate stained). Apical cells possess microvilli and cilia whereas the basal cells have only microvilli projecting into the lumen. The plane of section is somewhat oblique. Note the very dense granules in both types of cells. *L*, lumen; *c*, cilia; *mv*, microvilli; *g₁*, granules in basal cells; *g₂*, granules in apical cells; *A*, apical cell; *B*, basal cell; *a*, apical nucleus; *V*, vacuoloid. $\times 4000$.

FIGURE 2 Conventionally prepared electron micrograph showing the luminal border of epithelial cells of the shell gland (preparation same as Fig. 1). Note the very dense granules. See Fig. 1 for legend. $\times 15,000$.

tioned nuclei and similar to the nucleolus in Fig. 5, the grazed nucleus did not deposit a peripheral dense ash border and the entire nuclear area appears uniformly dense across its diameter. A light clear zone is visible around the periphery of the tangentially sectioned nucleus, although this is clearer in other spodograms (not shown).

Since the halos surrounding nuclei and nucleoli were never observed in unincinerated sections (Fig. 1), they were created during incineration. It is likely that they were formed by a contraction or shrinkage phenomenon during ashing. The widths of the halos shown in Figs. 3, 4, and 5 are typical for 0.5μ sections. It will be shown below that

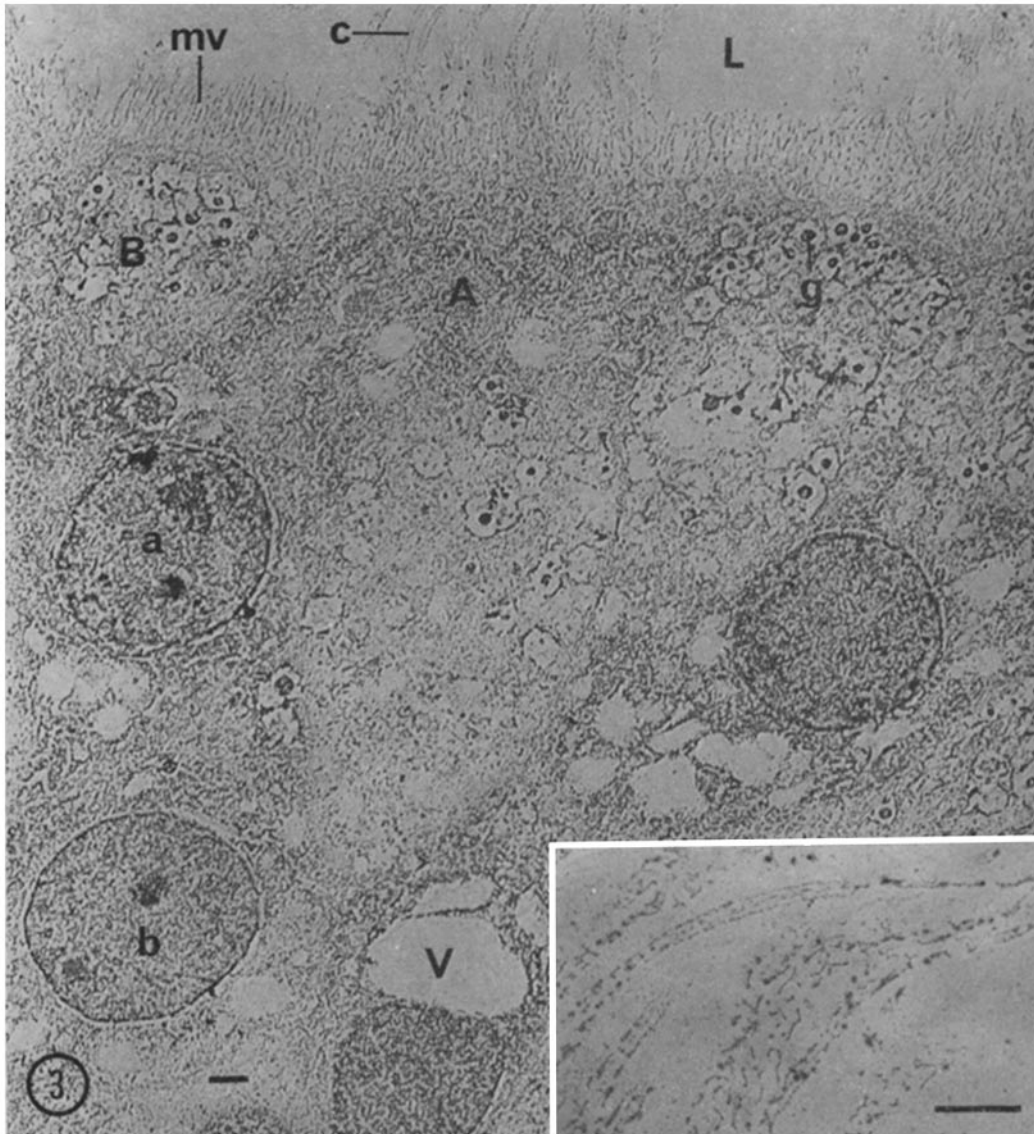


FIGURE 3 The remainder of the electron micrographs in this study (Figs. 3-31) show tissues after low temperature incineration. Fig. 3 shows the ash residue from glutaraldehyde fixed shell gland epithelial cells (0.5μ section). Note that cell membranes cannot be observed in the ash residue (compare with Fig. 4). See Fig. 1 for legend. $\times 5000$. *Inset*: Preparation same as Fig. 3: Detailed view of low temperature ashed cilia. $\times 11,000$.

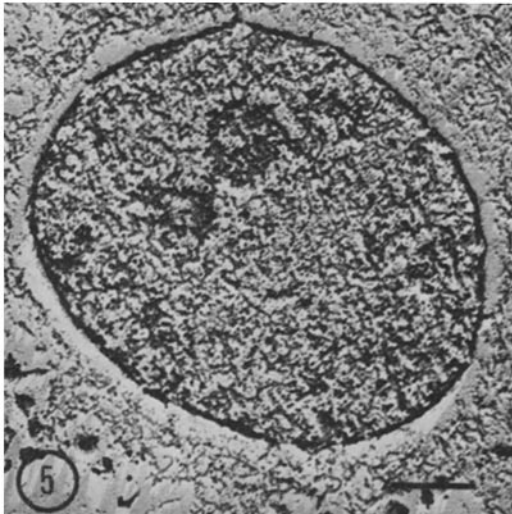
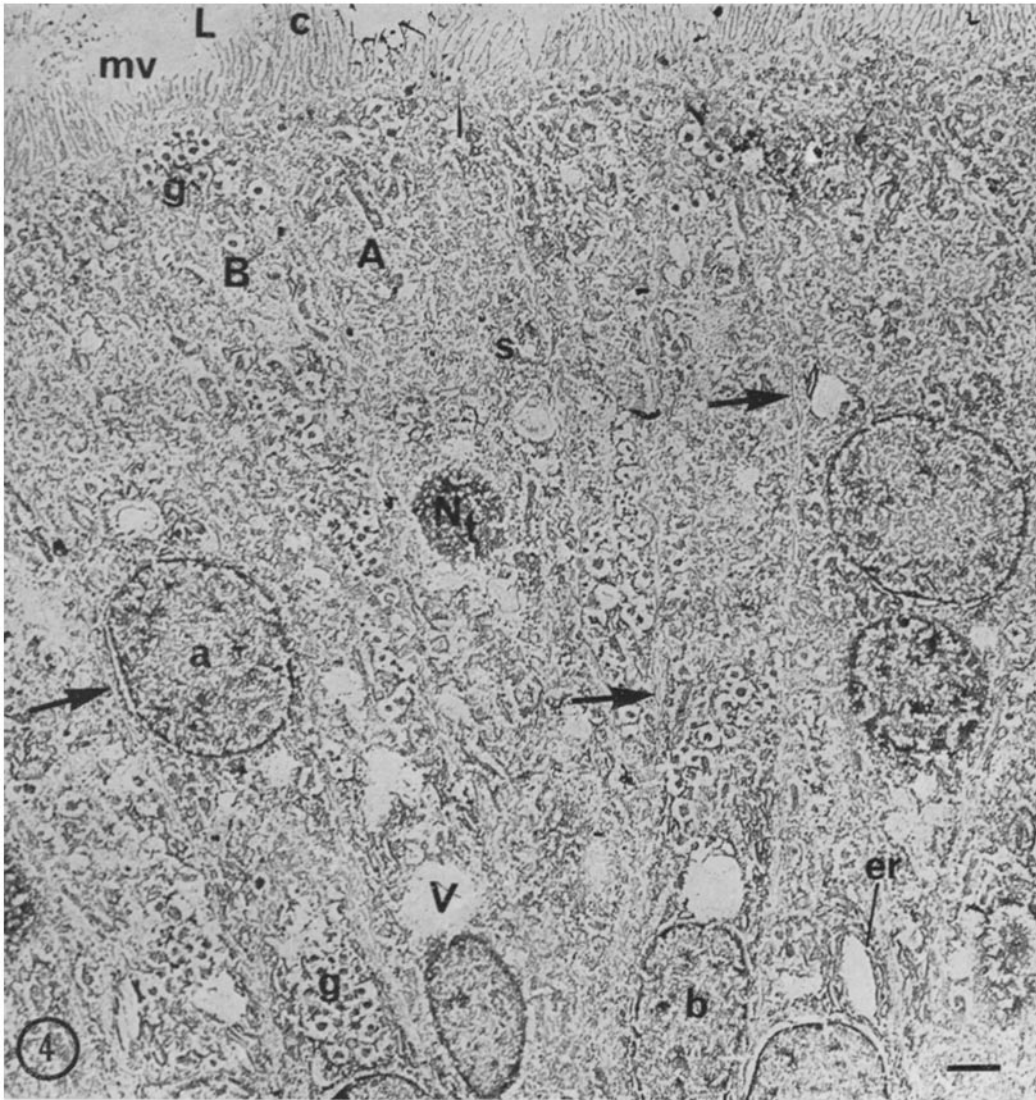


FIGURE 4 Glutaraldehyde fixed, osmium postfixed, incinerated, shell gland epithelial cells (0.5μ section). Note ash residues from cell membranes (arrows). See Fig. 1 for legend. N_t , tangentially sectioned nucleus; *er*, endoplasmic reticulum. $\times 5000$.

FIGURE 5 Glutaraldehyde fixed epithelial cell nucleus (0.5μ section, platinum shadowed). $\times 12,000$.

thicker sections yield wider halos and thinner sections yield narrower halos. Thicker sections seemed to be more susceptible to migratory forces as the organic material was removed during incineration. The ash strands observed within the clear zones in some places probably are remnants of incomplete migration.

This migration phenomenon raises the question of whether the dense ash borders around cross-sectioned nuclei were from mineral-rich material or were artificially formed during incineration. Although part of the ash borders may have formed from ash migration, it appears that the nuclear membrane region is truly mineral-rich for the following reasons: (a) tangentially sectioned nuclei did not form dense borders although they also contracted to leave clear zones (Fig. 4), (b) tangentially sectioned nuclei deposited very dense ash across their entire areas as though a broad area of only dense nuclear membrane was exposed by the oblique cutting angle, (c) similar to the grazed nuclei, nucleoli also deposited dense ash residues without formation of dense borders but with formation of clear zones, and (d) the nuclear borders in conventional micrographs are dense (Fig. 1) from cross-sectioned nuclei but not from tangentially sectioned nuclei or nucleoli. These observations favoring a mineral-rich nuclear membrane region were noticed consistently throughout this study.

The very dense granules (g_1 and g_2) that were noted in the conventional micrographs (Figs. 1 and 2) also deposited dense residues (g) after ashing as shown in the low magnification spodograms in Figs. 3 and 4. A more detailed view of the granules is shown in Fig. 6, a spodogram from shell gland tissue fixed in glutaraldehyde only, sectioned at about 0.5μ , ashed, and shadowed with platinum. The granules appear as small dense masses located approximately in the center of wide, circular clear zones. The appearance of the ashed granules contrasts with that of the unashed granules (Figs. 1 and 2) which are larger and not surrounded by clear zones. The ash residues appear either as solid, roughly spherical masses or as doughnuts with small electron-transparent regions near their centers. The height and shape of the ashed granules as revealed by shadowing shows that they are lumps of ash rather than flat, circular disks. The granule residues are approximately 2500 Å in diameter and about 700 Å high. To prove that the density of the ash was not caused by the platinum shadowing, the granules' inherent density is shown in Fig. 7 which is unshadowed. Finally, Fig. 8

shows the appearance of granules from osmium postfixed tissue after incineration. It is interesting to note that the granules from the osmium postfixed tissue (Fig. 8) actually appear less dense than those fixed only in glutaraldehyde (Fig. 7).

It is reasonable to assume that the origin of the clear zones around the granules is similar to that described for the nuclei. Note the distinct clear zones around the granules and their internal dense masses in Fig. 6. The original granules probably contracted during ashing to form the observed concentrated residues, leaving the surrounding area empty. The granules in the spodograms are labeled with the letter g without subscripts because the features that distinguished the two types of granules (g_1 and g_2 in Figs. 1 and 2) in apical and basal cells, respectively, were destroyed during low temperature ashing by the contraction phenomenon. The locations of some granules imply their origin as, for example, those in Fig. 8 which are within a basal cell distinguished by microvilli and the absence of cilia. It is not possible to distinguish the two granule types by examining only their ash residues.

In addition to the granules along the luminal border and scattered throughout the cells, it was mentioned above that granules also cluster on the luminal side of basal nuclei (see the labeled granule cluster near the bottom of Fig. 4). Detailed views of these basal granules are shown in Fig. 9 (glutaraldehyde fixed, shadowed) and Fig. 10 (glutaraldehyde fixed, unshadowed). Basically, the granules appear the same as already described, dense masses within clear zones. Fig. 9, however, shows two types of ash residues: small, dense, solid-appearing, contracted masses and larger, less dense, asteroid-appearing, less contracted masses. The smaller, more dense masses cast longer shadows and have wider clear zones than the larger, less dense masses. Therefore, it is likely that two different degrees of contraction are represented (incomplete ashing perhaps) rather than two separate species of granules. The observation of two types ash residues from granules was uncommon. The adjacent nucleus in Fig. 9 shows a space almost devoid of ash in the same relative location as the granules just described. Such empty spaces have been termed vacuoloids by Breen and De Bruyn (1969) because there are no limiting membranes around them. This term distinguishes vacuoloids from membrane-bounded vacuoles. The absence of a limiting membrane is reflected clearly in the ash pattern. Vacuoloids (V) are also

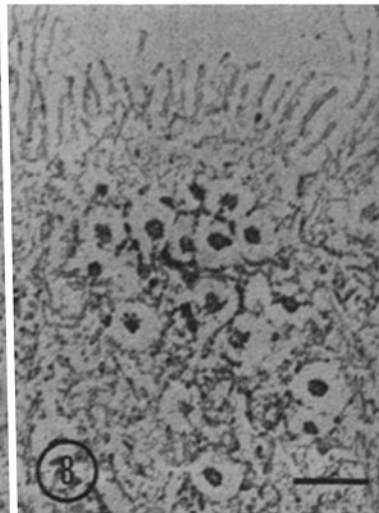
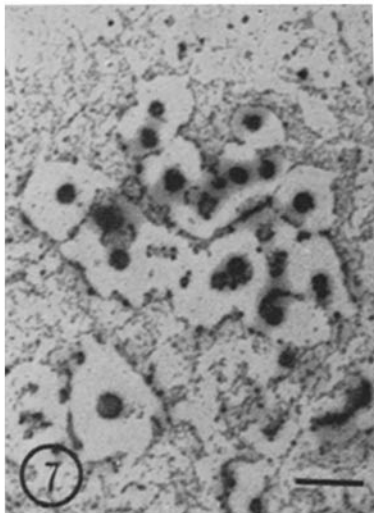
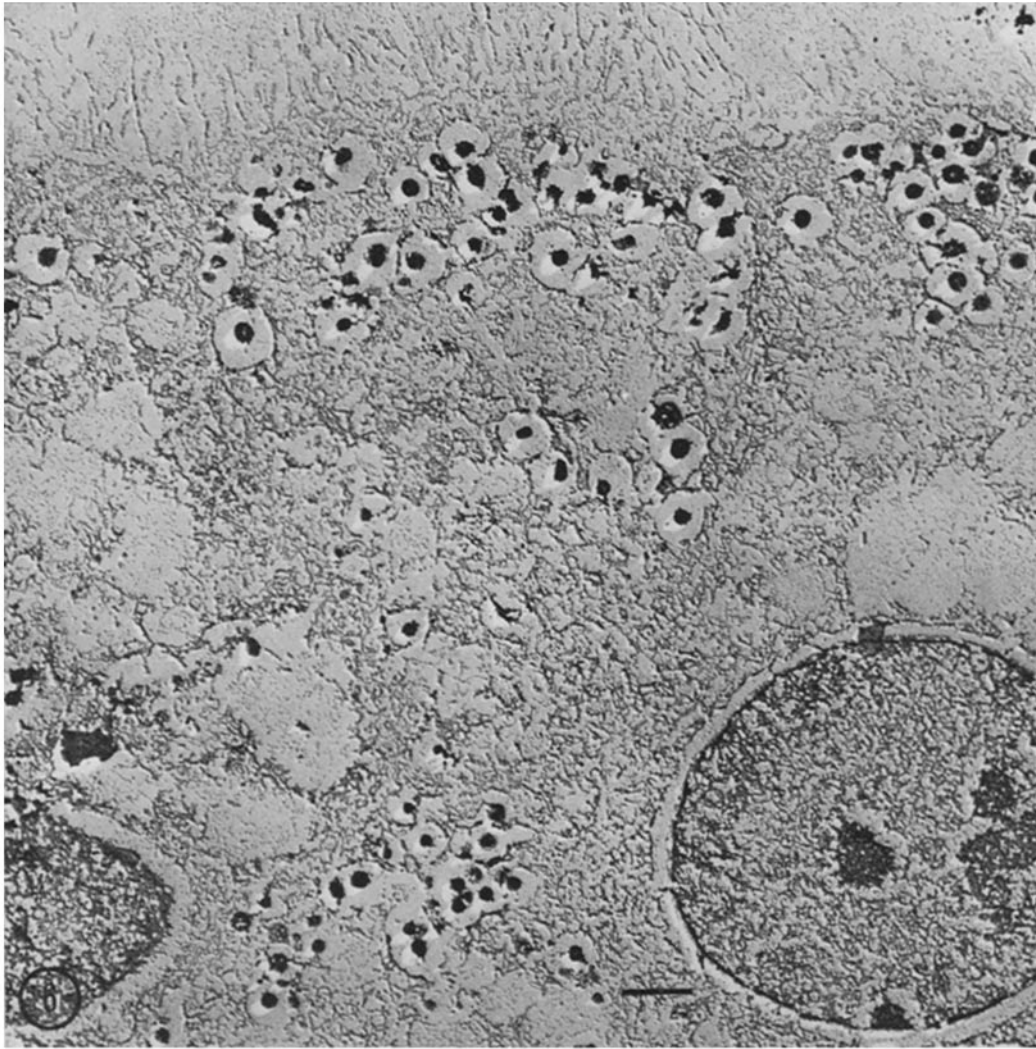


FIGURE 6 Ash residue from granules near the luminal border in glutaraldehyde fixed epithelial cells after low temperature incineration (0.5μ section, platinum shadowed). $\times 9000$.

FIGURE 7 Similar to Fig. 6 except unshadowed. $\times 9000$.

FIGURE 8 Similar to Fig. 6 except from osmium postfixed tissue and unshadowed. $\times 10,000$.

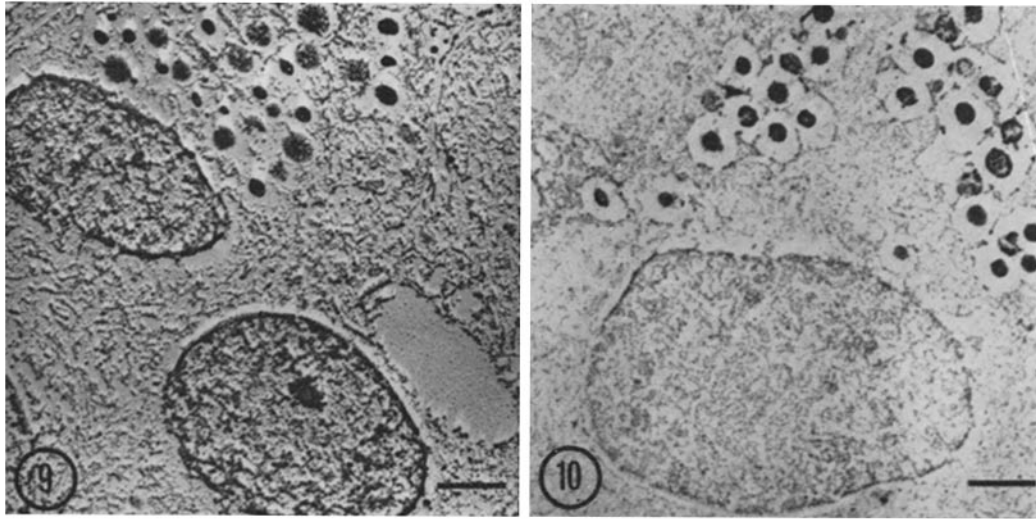


FIGURE 9 Two basal nuclei, one with granules and the other with a vacuoloid, in the luminal cytoplasm (glutaraldehyde fixed, 0.5μ section, platinum shadowed). $\times 9000$.

FIGURE 10 Similar to Fig. 9 except unshadowed. $\times 9000$.

present in Figs. 3 and 4. It was not possible to determine the significance of the small amount of material within the vacuoloids. Once again, note the clear zones around the nuclei in Fig. 9. This same relative site, the luminal side of basal nuclei, is sometimes filled with endoplasmic reticulum. An example of this, with several granules, is shown in the spodogram of Fig. 11 (glutaraldehyde fixed, shadowed). Not only are granules, vacuoloids, or endoplasmic reticulum seen in this site, but combinations of two or three of these sometimes are observed at the same time. Fig. 12 shows a large vacuoloid with remnants of endoplasmic reticulum and a few granules remaining in the ash next to one nucleus; endoplasmic reticulum, a small vacuoloid, and a few granules are next to the adjacent nucleus. Similar examples are included in Figs. 3 and 4. These observations suggest that there could be cyclic transitions from one state to another. Johnston et al. (1963) and Breen and De Bruyn (1969) have postulated that this site next to basal nuclei undergoes intense activity related to the function of these cells. For the purposes of this study, it is sufficient to note the degree of detail and complexity that the low temperature ashing technique is capable of revealing.

One additional view of the active site in basal cells is shown in Fig. 13 which shows a large vacuoloid with laterally displaced endoplasmic

reticulum in the center and granules next to another vacuoloid in the lower left. This spodogram is included because the section thickness (about 0.2μ) was thinner than that of the other spodograms thus far described (Figs. 2-12), and the sample shown was viewed in the electron microscope before incineration. The significance of the relatively thin section is that much greater detail remains in the ash pattern. Note that the granules are not contracted into dense masses and that there is no clear zone around them. They appear to have retained the same dimensions seen in Figs. 1 and 2. The nuclei and their dense interior regions also lack the clear zones characteristic of the 0.5μ sections. The endoplasmic reticulum is very clearly defined in the ash pattern. The significance of the previewing is that this step results in a peculiar "muddy" appearance. This effect is especially noticeable within the vacuoloid in Fig. 13 because this area is nearly ash-free. Although not fully understood, it appears that a contamination layer was formed during exposure to the electron beam. Subsequent ashing evidently was not severe enough to remove the contamination. Adjacent areas of the same grids that were not exposed to the electron beam did not have the muddy appearance and showed normal ash patterns. There is some question whether the enhanced detail of Fig. 13 is preserved because the section is thin or because

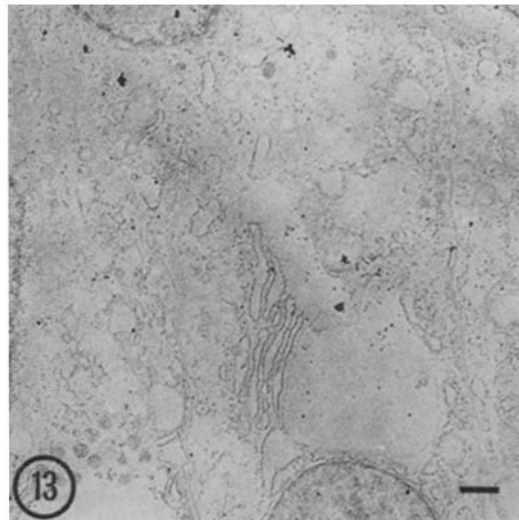
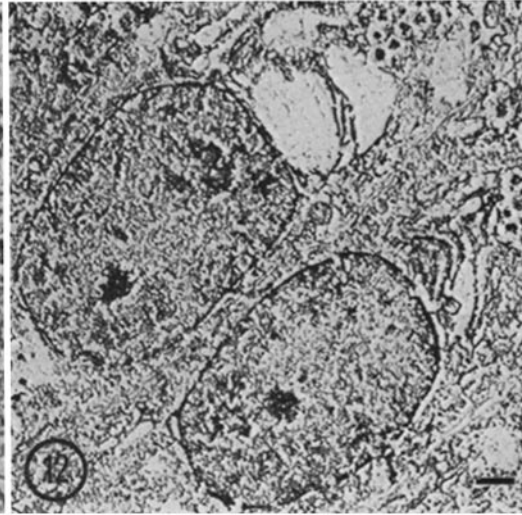
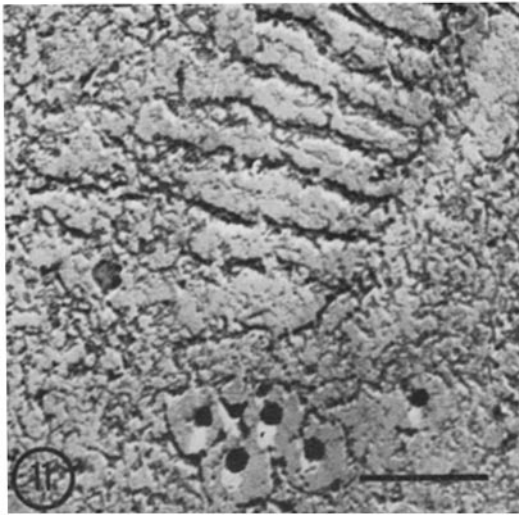


FIGURE 11 Granules and endoplasmic reticulum located in the luminal cytoplasm adjacent to a basal nucleus (glutaraldehyde fixed, 0.5μ section, platinum shadowed). $\times 17,000$.

FIGURE 12 Basal nuclei with vacuoloids, endoplasmic reticulum, and granules all present at the same time in various degrees in the luminal cytoplasm of basal epithelial cells (glutaraldehyde fixed, osmium postfixed, 0.5μ section, platinum shadowed). $\times 5000$.

FIGURE 13 Ash residue from the luminal cytoplasm adjacent to basal nuclei showing a large vacuoloid with displaced endoplasmic reticulum in one cell and granules near a vacuoloid in an adjacent cell (glutaraldehyde fixed, osmium postfixed, 0.2μ section). Unlike Figs. 3-12, this section was thinner and was viewed before incineration. $\times 5000$.

incineration was incomplete due to the contamination layer. It is difficult to separate the two effects. However, nonpreviewed thin sections also demonstrate similar detail as will be illustrated below. The entire study was not done with thin sections (rather than the usual 0.5μ sections) because spodograms such as that shown in Fig. 13 represent the lower limit of what is visible in the electron microscope. The black particles in Fig. 13 were used to relocate this previewed site after incineration. Thin sections are very useful but very difficult to use (see Boothroyd, 1968).

Another prominent feature of the conventional micrographs in Figs. 1 and 2 is the mitochondria. Generally, mitochondria are not identifiable after ashing 0.5μ sections as seen in Figs. 3 and 4.

Careful inspection may reveal mitochondrial ash, but such residues are not clear. One rare example of ash recognizable as originating from mitochondria in a 0.5μ section is shown in Fig. 14 which was osmium postfixed. When thinner sections were low temperature ashed, mitochondria with cristae were readily recognizable in the ash patterns as illustrated in Fig. 15. Comparison of the mitochondria in Figs. 14 and 15 offers another demonstration of greater distortion in thicker sections (Fig. 14) and better resolution in thinner sections (Fig. 15). A few mitochondria also may be seen in Fig. 13 since it was from a thin section. These illustrations show that thin sections are essential if mitochondrial preservation is desired.

Figs. 1 and 2 show various sizes of true vacuoles

(as distinguished from vacuoloids) scattered throughout the cells. Such relatively clear areas are reflected in the ash patterns after incineration as shown in Figs. 3 and 4. Vacuolization can become very extensive, particularly in the apical cells, which raises many possibilities regarding their secretory role, but the absence of prominent ash deposits in or around vacuoles makes them of limited interest from the viewpoint of micro-incineration.

Microvilli (mv) from both apical and basal cells and cilia (c) from only apical cells are observed projecting into the shell gland lumen (L) in micrographs from both the unashed (Figs. 1 and 2) and ashed (Figs. 3 and 4) tissue. The micrographs of unashed tissue show more cross-sections of these projections, whereas those of the ashed tissue show more longitudinal sections. Detailed examination of the ashed microvilli (Figs. 3 and 4) shows that the ash residues lie in parallel, discontinuous rows which presumably were deposited from the limiting membranes. Cilia are distinguished from the microvilli in the ash by their greater length and width (see Inset, Fig. 3). In favorable longitudinal sections, an additional parallel row of ash is observed in the central core of cilia. This core ash is double in one of the cilia shown in the inset of Fig. 3. The spaces between these rows of ash appear devoid of ash. Presumably, this ash pattern arose from the characteristic filamentous 9 + 2 tubule arrangement of cilia as shown in Figs. 1 and 2.

It was noted that Fig. 3 was prepared from tissue fixed only in organic fixative (glutaraldehyde) and that Fig. 4 was prepared in the same way but with the addition of osmium fixation. Comparison of the spodograms from these two methods yields strikingly similar results. In Figs. 3 and 4, note that most of the features recognized in one preparation were observed in the other. However, there is one clear exception: lateral cell membranes (shown unashed in Fig. 1) were observed consistently in the ash from osmium postfixed cells (arrows, Fig. 4) and were absent in the ash from glutaraldehyde-only fixed cells (Fig. 3). This membrane ash also may be seen in all the other osmium postfixed spodograms which include adjoining cells (Fig. 8, left edge; Fig. 12, between the nuclei as well as on either side of them; and Fig. 13, especially distinct in this thin section). The membrane ash is not recognizable in any of the micrographs from glutaraldehyde-only fixed tissue (Figs. 3, 6, 7, 9, and 10). A higher magnification, platinum shadowed view of the cell boundaries separating

three cells in osmium postfixed tissue is shown in Fig. 16. The ash from the lateral membranes (arrows) appears as discontinuous, double, parallel rows along most of their length. A small invagination is apparent along one membrane. It seems that osmium does enhance the appearance of ash residues from certain membranous structures, yet the over-all quantity of ash does not seem to be increased by the osmium. Another possible example illustrating this point is the observation that the membranes of mitochondria as shown in Figs. 13, 14, and 15 all were from osmium postfixed tissue. From these examples it can be seen that the addition of osmium does not introduce gross differences but rather differences in detail which can be observed from careful examination of the ash patterns. Whether the osmium remains in the ash from the lateral membranes and mitochondria or whether it only influences the pattern of the ash deposit and is volatilized (and thus removed) from the tissue during incineration cannot be determined at this time (see Discussion).

Finally, Figs. 3 and 4 show large cytoplasmic areas that definitely contain ash but do not show recognizable structures. Part of this ash is from the cell substructures which have become too distorted to be recognized at this section thickness (mitochondria, for example). It is notable how ubiquitously ash is deposited throughout the tissue. There are no completely "empty" regions, with the possible exception of vacuoloid and vacuole interiors which are very susceptible to mineral loss during aqueous preparation. High temperature ashing shows comparable cytoplasmic regions to be more devoid of ash and relatively featureless (see Boothroyd, 1968; Thomas, 1969).

GLAND CELLS: The tubular glands are located in the shell gland mucosa below the lining epithelium. A single gland consists of a central lumen surrounded by gland cells. A cross-section of approximately half of one gland is shown in Fig. 17 which was osmium postfixed and sectioned at approximately 1.0μ . As in the case of the epithelial cells, nuclei were the most prominent features in the ash of gland cells. Note the very wide circum-nuclear zones in this spodogram, an observation consistent with the thickness of the section. Fig. 17 was from a section two times thicker than those in Figs. 2-12 and Fig. 14 and five to ten times thicker than those in Figs. 13 and 15. Also due to the section thickness, the cytoplasmic ash is very distorted. Within the lumen there appears to be a

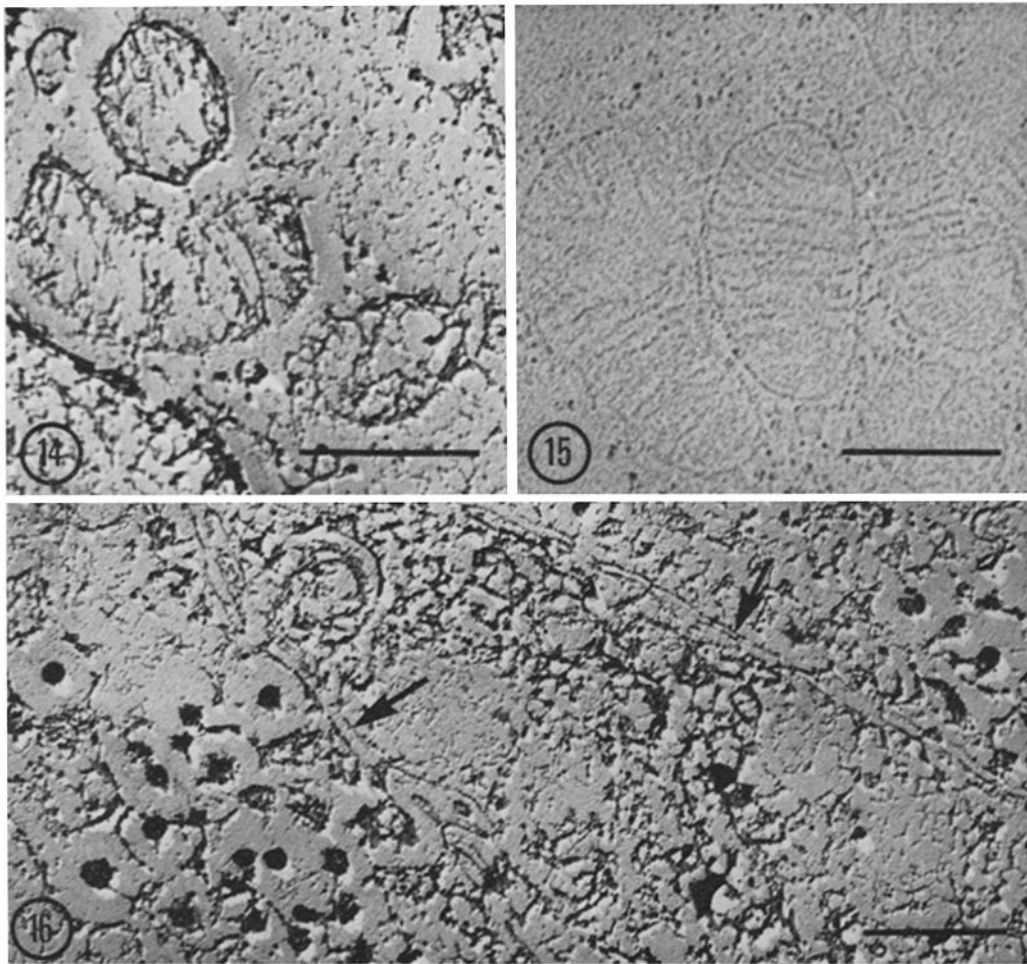


FIGURE 14 Ash residue from shell gland mitochondria (glutaraldehyde fixed, osmium postfixed, 0.5μ section, platinum shadowed). The mitochondrial ash is more commonly unrecognizable in 0.5μ sections. $\times 24,000$.

FIGURE 15 Ash residue from shell gland mitochondria in a thin spodogram (glutaraldehyde fixed, osmium postfixed, about 0.1μ section). $\times 21,000$.

FIGURE 16 Ash residue from lateral cell membranes (arrows) between glutaraldehyde fixed, osmium postfixed, shell gland epithelial cells (0.5μ section, platinum shadowed). The shell gland lumen is beyond the upper left of micrograph. $\times 19,000$.

relatively uniform ash deposit of unknown significance. The remains of microvilli line the lumen in Fig. 17 and are shown in more detail in Fig. 18 (osmium postfixed, 0.5μ section). Some of the microvilli were longitudinally sectioned as indicated by parallel rows of ash; others were cross-sectioned. Perhaps the most significant feature of the gland cells is that clusters of distinct granules as shown in epithelial cells were not observed. Vac-

uoles were a more prominent feature in these cells (also see Johnston et al., 1963). Some individual gland cells occasionally have been observed to be relatively ash-free while adjacent cells exhibit typical appearances (see Schraer and Schraer, 1970, Fig. 5). The absence of mineral concentrations in the form of granules in gland cells could contribute to determining the ultimate role of these cells.

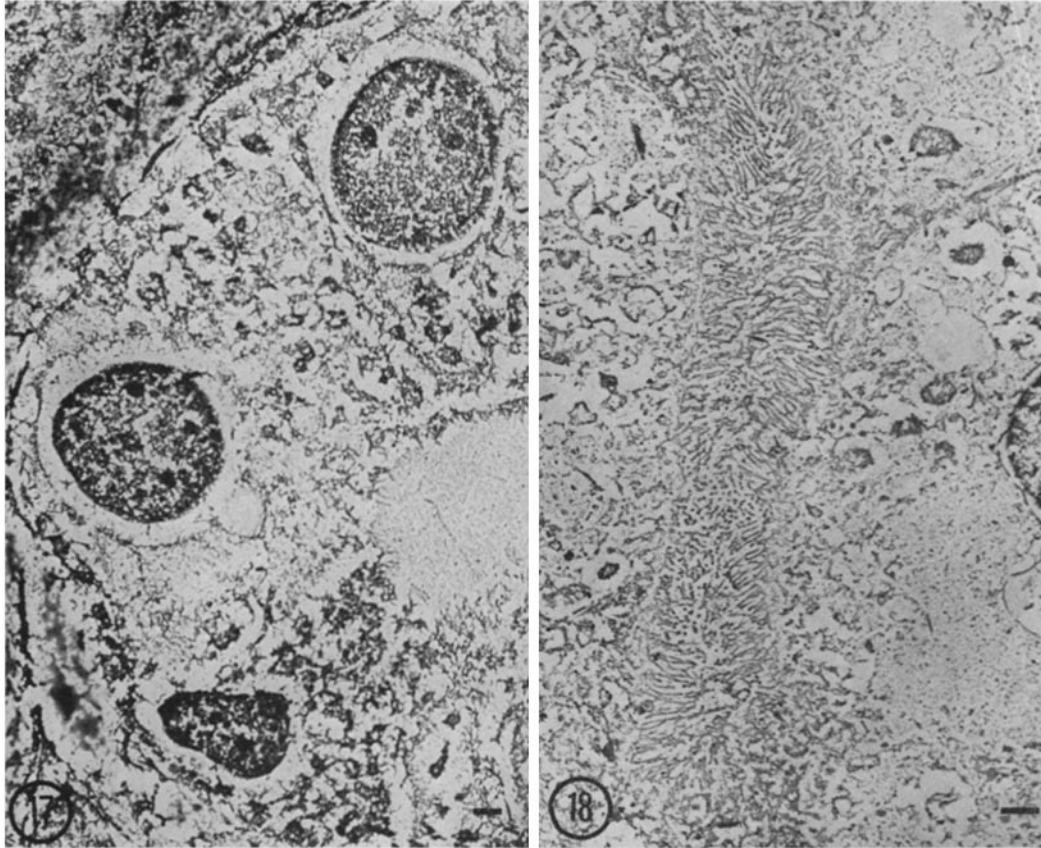


FIGURE 17 Glutaraldehyde fixed, osmium postfixed tubular gland cells (1.0μ section). $\times 4000$.

FIGURE 18 A longitudinally sectioned tubular gland lumen showing microvilli. Preparation similar to Fig. 17 except the section was 0.5μ thick. $\times 5000$.

Erythrocytes and Collagen

In addition to the epithelial and gland cells of the shell gland mucosa, erythrocytes and collagen were examined after low temperature incineration.

ERYTHROCYTES: Erythrocytes, which are nucleated in birds, were observed within capillaries interspersed between the tubular glands and adjacent to the columnar cells (Schraer and Schraer, 1971). An osmium postfixed, 0.5μ , low temperature incinerated red blood cell is shown in Fig. 19. The extremely dense ash deposits from the nucleus contrasts with the lighter, homogeneous, fibrous ash from the cell cytoplasm. The densest portions of the nuclear deposits are located around the periphery and in the center of the nucleus. A sparse ash is distributed in the spaces between the dense deposits. The nucleus is encircled by a clear

zone similar to that described for nuclei, nucleoli, and granules within the mucosal cells. The whole cell boundary also has a clear zone around most of its periphery. These clear zones probably are manifestations of ash migration as described below.

Since the erythrocyte nuclei from 0.5μ sections produced such dense ash residues, these cells were particularly favorable for low temperature incineration of thin sections. Fig. 20 is an example of a glutaraldehyde fixed, thin sectioned (about 0.1μ), low temperature ashed nucleus. Only the nucleus is shown in this spodogram because the limiting boundary of the whole cell could not be defined in this thin section. Note that only the organic components were used in preparing this sample. As in Fig. 19, the ash residue is organized in discrete masses separated by large spaces which contain little or no ash. The dense nuclear masses contain

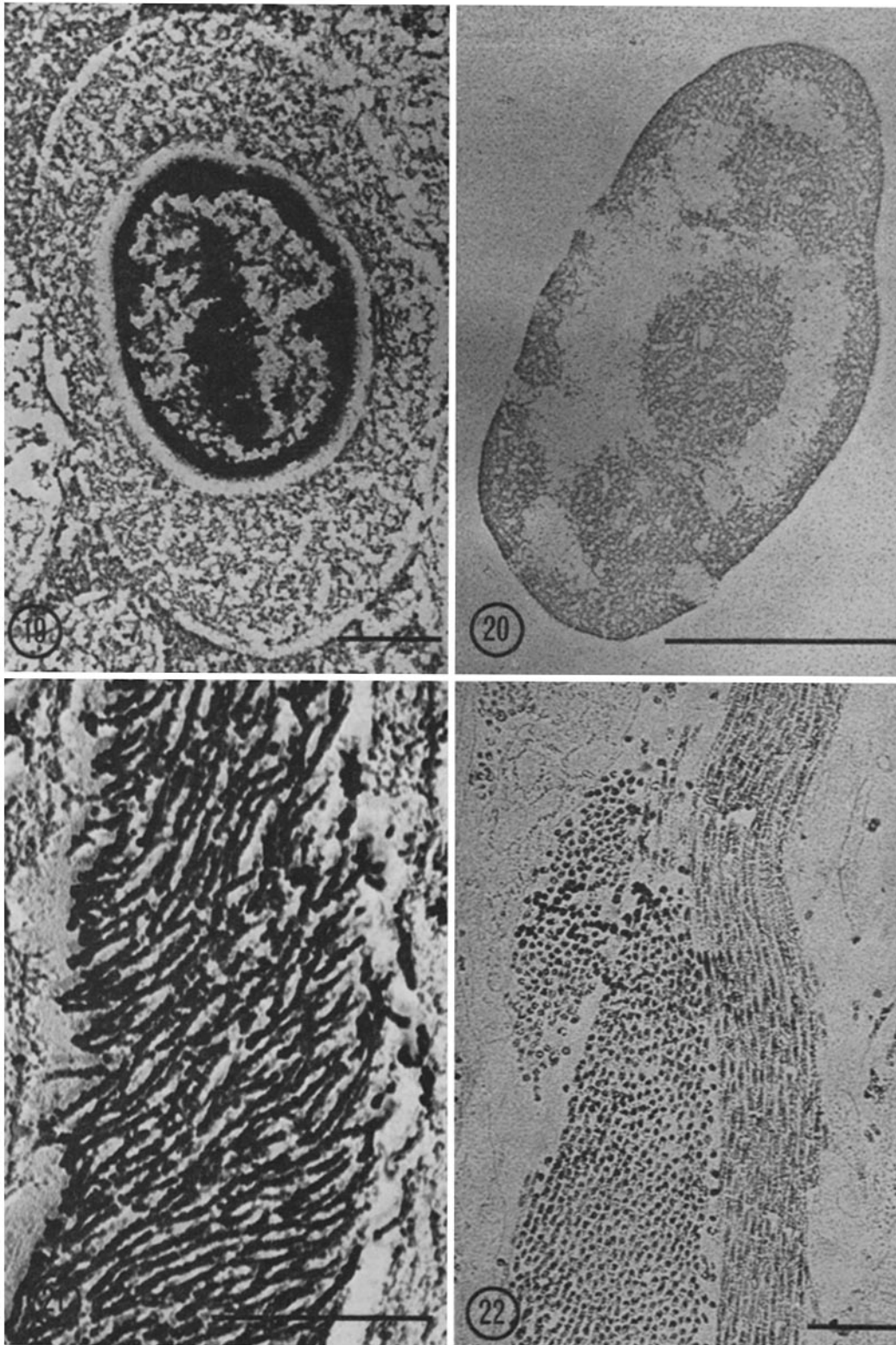


FIGURE 19 Shell gland erythrocyte (glutaraldehyde fixed, osmium postfixed, 0.5μ section). $\times 16,000$.

FIGURE 20 Shell gland erythrocyte nucleus (glutaraldehyde fixed, about 0.1μ section). $\times 36,000$.

FIGURE 21 Shell gland collagen (glutaraldehyde fixed, 0.5μ section, platinum shadowed). $\times 34,000$.

FIGURE 22 Shell gland collagen (glutaraldehyde fixed, osmium postfixed, about 0.1μ section, unshadowed). $\times 14,000$.

small, indistinct, clear areas. Around the outer periphery of the nucleus there is a clearly defined ash border which is discontinuous in some places. Generally there is no dense ash material within or opposite these breaks. The obvious ash migration that caused the wide clear zones in Fig. 19 is not apparent in this thin section.

COLLAGEN: The ash from collagen was observed in the connective tissue between tubular glands. Fig. 21 is a glutaraldehyde fixed, 0.5 μ , shadowed example of incinerated collagen that shows easily recognizable ash deposits with suggestions of segmentation. Thin sections show much more detail as in Fig. 22 which is osmium postfixing, 0.1 μ thick, and unshadowed. Longitudinal sections show distinct segmentation of the collagen fibers and cross-sections show many hollow centers.

Special Treatments and Technical Considerations

STAINING: Since most stains are heavy, electron-opaque metals, they usually are nonvolatile when subjected to low temperature incineration. For this reason a brief experiment was performed in this study to explore the potentials of this technique for studies of stain-binding sites. Figs. 23 and 24 are shell gland mucosal cells which were fixed in

osmium (without glutaraldehyde prefixation), thin-sectioned, stained with lead citrate, and low temperature incinerated. Fig. 23 is from a thin section (probably less than 0.1 μ) that shows very fine details such as nuclear membranes, plasma membranes, and endoplasmic reticulum remaining after low temperature ashing. The parallel rows of ash from the plasma membranes offer a dramatic example of the excellent resolution obtainable from thin sections. No contraction or shrinkage (ash migration) of the nucleus occurred in this thin section as indicated by the absence of a halo. Ash residues from such thin sections were barely visible on the fluorescent screen of the electron microscope. Fig. 24, a slightly thicker spodogram, shows mitochondria preserved in the ash between two nuclei. Granules, such as those in Figs. 1 and 2, appear as groups of closely packed grains with no evidence of contraction or ash migration after ashing lead-stained material (not illustrated). Comparison of the lead-stained and the unstained sections showed one puzzling difference: the nuclei have a relatively homogeneous appearance in the lead-stained spodograms in contrast to the variable densities shown throughout this paper. This use of low temperature ashing was not pursued further, but it is presented as an example of a tool that could be used to approach many questions con-

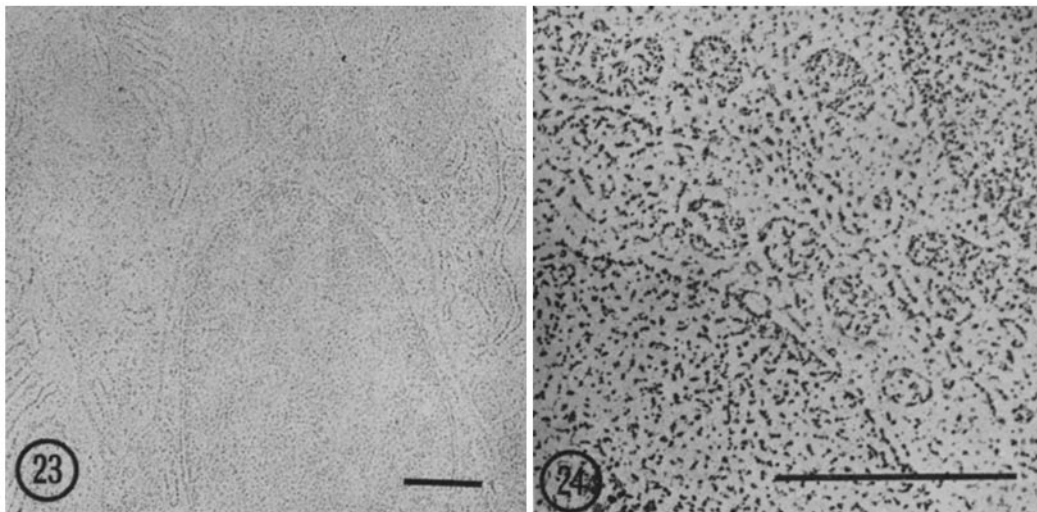


FIGURE 23 Ash residue from lead-stained shell gland epithelial cells (osmium fixed, less than 0.1 μ section). $\times 10,000$.

FIGURE 24 Ash residue from lead-stained mitochondria between two shell gland epithelial nuclei (osmium fixed, about 0.1 μ section). $\times 15,000$.

cerning stains and the structures to which they bind. As an added note, it was discovered that unstained erythrocyte sections exposed to the electron beam would not subsequently accept the stain.

SHADOWING: Comparison of electron micrographs of preshadowed and postshadowed specimens showed no observable alteration of the ash patterns caused by the shadowing procedure. Even delicate strands of ash from grossly distorted ash samples which had little contact with the support film were undisturbed. Shadowing was not essential to enhance contrast, but it was useful for studying the three-dimensional shape of residues.

PREVIEWING: An attractive feature of ultramicroincineration is that specimens may be previewed before incineration and reviewed after incineration to gain orientation and origins of the ash deposits. However, previewing is attended by several problems that hinder, but do not necessarily prevent, its use. First, only thin sections can be previewed. Second, previewing sections from which stains and heavy metals have been purposefully omitted is difficult due to low contrast. Third, the electron beam alters the specimen as demonstrated by the previewed erythrocytes which would not subsequently accept the stain. Fourth, previewed areas sometimes are destroyed before postviews are obtained. Finally, contamination from the electron beam imparts the muddy appearance to the electron micrographs as noted in Fig. 13 (see Thomas, 1969). Figs. 25 and 26 show examples of preview and postview micrographs from an identical site on a grid. Some contrast is evident in the preview (Fig. 25) because the tissue was postfixed in osmium. The indistinct muddy appearance is very evident in Fig. 26. Apparently, the mild low temperature ashing conditions were sufficient to ash an unpreviewed sample but not to remove contamination. The contamination does not totally shield the specimen from the excited oxygen because the postview micrographs are quite different from the previews. Comparing Figs. 25 and 26, the ashing preserved some features such as mitochondria, vesicles, and membranes; however, it also brought out a large dense area within the nucleus that was not visible before ashing. In view of the problems, previewing is not as advantageous as anticipated; however, it is useful if the limitations are recognized.

COMPLETENESS OF ASHING: Classical tests for completeness of ashing, such as color or solubility in acid, are not practical at the ultramicroincineration level. In this study, samples were

assumed to be ashed completely when the ash pattern from two sequential incinerations appeared identical in the electron microscope. Fig. 27 shows an example of an incompletely ashed thick section. The very dense, solid appearing portions are the unashed material. Repetition of the ashing time yielded the spodogram in Fig. 28. The unashed portions seen in Fig. 27 were completely ashed in Fig. 28, whereas the completely ashed portions in Fig. 27 remained unchanged in Fig. 28. Using this procedure, the conditions employed in this study were determined to be greater than required for complete ashing.

Complete ashing was dependent upon the sample position within the oxidation chambers since incineration did not occur uniformly throughout the chambers of the asher. The relative oxidation rates of various sections of the chambers were determined by exposing carbon-coated glass slides to the stream of excited oxygen and noting the locations on the slides which oxidized most rapidly. For the Tracerlab LTA-600 used in this study, this position was determined to be at the center of the slides about 2.5 cm from the chamber door.

RESOLUTION: Section thickness and its effect on resolution has been noted several times in the descriptions of the spodograms presented in this study. Very thin sections (Figs. 13, 15, 20, 22, 23, 24, and 26) yield good resolution in which ash migration is minimal. Thicker sections of about 0.5 μ (Figs. 3-12, 14, 16, 18, 19, and 21) show much less detail than the thin sections and evidence of ash migration in the form of clear zones (halos) around nuclei and granules. More distortion and wider clear zones are evident from 1 μ sections (Fig. 17) and from 1.5 μ sections (Figs. 27 and 28). An ashed 2 μ section is shown in Fig. 29. Severe distortion is indicated by the very wide clear zones. Clear zones up to 12,000 \AA wide were observed around shrunken nuclei from 2 and 4 μ sections. Extreme examples of ash migration occurred when specimens had poor or no contact with the support films, such as when folds in the sections were ashed (Fig. 30). As can be seen, the ash is extremely distorted, curled, fragmented, and sometimes in the form of thin wisps rising from the support film. An obvious rule emerged from these observations: the thinner the section, the better the resolution.

ELECTRON MICROPROBE ANALYSIS: The useful information from electron microprobe analysis resulted from traversing osmium postfixed, 0.5 μ , incinerated sections under a minimized static

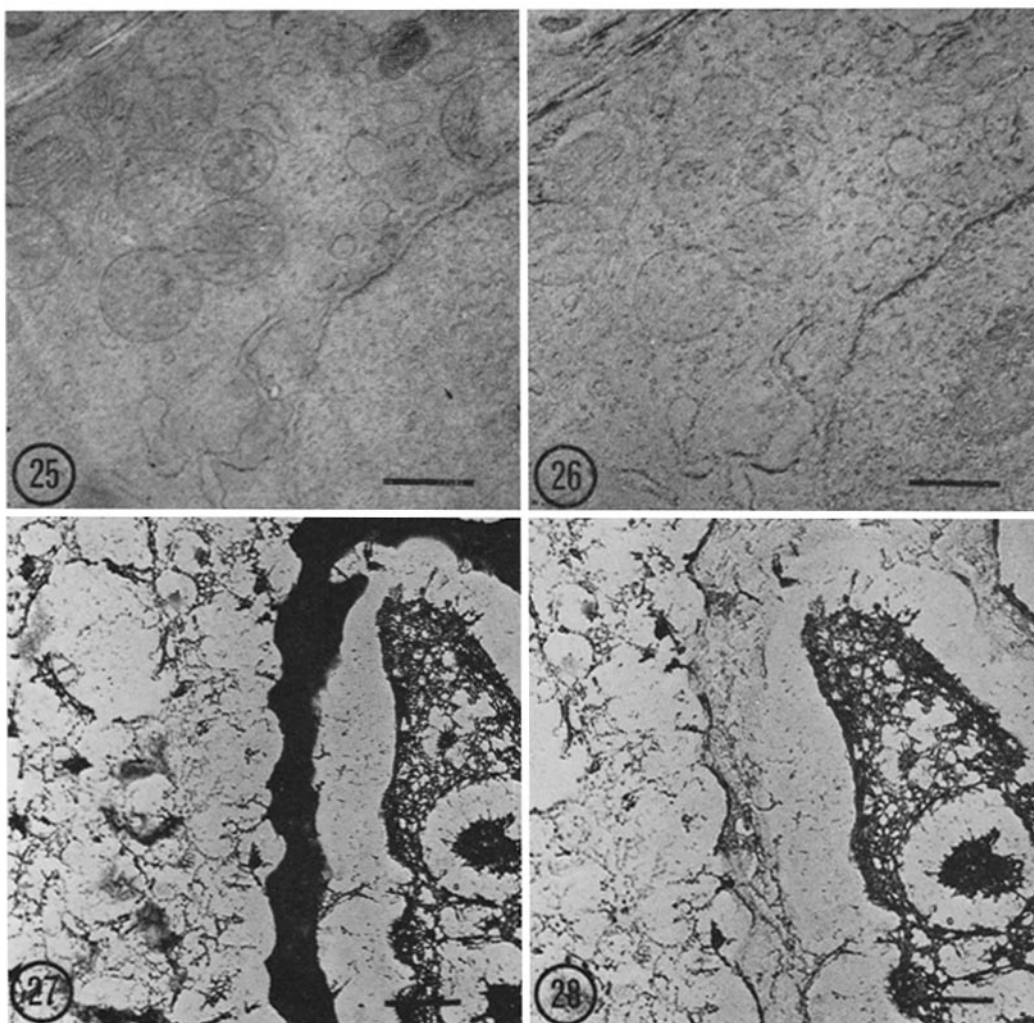


FIGURE 25 Preview of a thin section that is unincinerated and unstained (glutaraldehyde fixed, osmium postfixed). The osmium has provided sufficient contrast to distinguish a nucleus, mitochondria, small vesicles, and membranes. Compare with Fig. 26. $\times 12,000$.

FIGURE 26 Postview of the identical site shown in Fig. 25 after low temperature incineration (preparation same as Fig. 25 except for the incineration). The nuclear membrane, mitochondria, vesicle boundaries, and membranes are recognizable in the ash from this thin section, but they are less distinct than the same structures in the unashed micrograph (Fig. 25). Note the appearance of a dense region (nucleolus?) in this postview that was not obvious in the preview. One dense body in the upper right of Fig. 25 almost disappeared in Fig. 26; another dense body in the upper left of Fig. 25 remains very dense in Fig. 26. The over-all "muddy" appearance due to specimen contamination by the electron beam is very noticeable, especially within relatively clear regions such as the vesicles and the nucleus (see text for more details). $\times 12,000$.

FIGURE 27 An example of incomplete incineration (glutaraldehyde fixed, 1.5μ section). The black, dense regions have not been ashed completely by the excited oxygen. Compare with Fig. 28. $\times 10,000$.

FIGURE 28 Identical site as shown in Fig. 27 after repeating the incineration. Note that the dense regions of Fig. 27 are completely ashed. Other regions that appeared completely ashed in Fig. 27 are unchanged after the repeated ashing in Fig. 28. $\times 12,000$.

spot (15 kv accelerating voltage, 0.02 μ amps specimen current) in an electron microprobe. Both strip chart recordings and scalar readouts detected low but significant levels of P and Ca X-ray emission. When the analyzed specimens were replaced in the electron microscope, dense tracks showed the precise pathway the microprobe beam had traversed (Fig. 31). Correlation of the numerical data from the microprobe and the visual information from the electron microscope showed that this method could distinguish the presence or absence of P and Ca in the tissue sections but it was not possible to locate P and Ca in specific subcellular structures. From these preliminary trials, it can be concluded only that P and Ca were present in the ash after low temperature incineration.

DISCUSSION

There are no known studies that can be compared directly with the present work on electron microscopy of thin-sectioned, low temperature incinerated, shell gland tissue. The incinerated shell gland tissue has been studied by Richardson in 1935, but this study used high temperature ashing, thicker sections, and light microscopy. Boothroyd (1968) has combined microincineration and electron microscopy but he used high temperature ashing and different tissues (rat epididymis and kidney cortex). Standard electron microscopy has well documented the unincinerated shell gland (see references in the Introduction). In spite of the differences between previous work and this study, comparisons yield some interrelated points.

The magnitude of detail preserved and revealed by low temperature ultramicroincineration was too great to permit a meaningful comparison with Richardson's high temperature, light microscope study. However, Richardson described dense "rings" of ash, granular aggregations of ash in apical cells, and a fine haze of ash along the luminal border which could have originated from nuclei, granules, and cilia, respectively, as described in this study. He also described clumps of ash which he attributed to cell "wall" or membrane origin, but it likely that this ash was derived from much more than cell membrane alone. Even with the low temperature technique, plasma membranes were clearly recognizable only in thin, osmium postfix sections. The many subcellular cytoplasmic details observed in this study, such as plasma membranes, endoplasmic reticulum, individual granules, vacuoles, mitochondria, etc.,

were, understandably, not recognizable in the high temperature, light microscope work. It is interesting that Richardson noted more irregularly distributed ash in the cytoplasm of the lining epithelial cells than in the relatively ash-free gland cells. This more detailed study led to essentially the same conclusion because the ash from the granules described in the Experimental Results was in epithelial cells. Such clusters of granules were not observed in the gland cells. Finally, Richardson was concerned with the same tissue processing problems in 1935 that are mentioned in this study. For example, he used a nonaqueous, organic fixative (alcohol formalin), floated his sections onto absolute ethanol or methanol to reduce mineral loss, and found that 5 μ was the maximum section thickness which preserved clear cytological details. For the same reasons, all organic solutions (except where noted) were used in this study. The use of aqueous solution necessarily limited this study to nonsoluble or structure-bound minerals.

Boothroyd's high temperature incineration work with the electron microscope is the study that is most closely related to this paper, yet many differences make comparisons difficult. Boothroyd used different ashing methods (550° C in air), tissues (rat epididymis and kidney cortex), section thicknesses (500–1200 A), buffers, embedding material (Araldite), techniques for support film preparation, etc. Realizing that some factors could be due to these differences in experimental conditions, the following contrasts between Boothroyd's study and this study are noted. Both studies showed high mineral content in nuclei and nucleoli. This was not surprising because Scott (1933) showed that dense ash from nuclei was common in many types of mammalian cells and that much of the ash was in the chromosomes and spindle areas of mitotic cells. Many other investigators (see Kruszynski, 1963) have studied the content of nuclear ash residues and have demonstrated the presence of Ca, Mg, P, K, and Fe. Boothroyd showed mitochondria as depositing little ash residue, whereas the mitochondrial ash was more detailed in thin sections in this work (although mitochondria were distorted beyond recognition in thicker sections). Boothroyd noticed that red blood corpuscles (rat) appeared to leave very little residue whereas the red blood cells in this study (chickens) deposited very dense residues. Boothroyd described dense ash from collagen, but the high temperature results did not show the easily identifiable segmentation which remained

after low temperature ashing. Richardson also noted that appreciable quantities of ash remained from "connective tissue fibers" in his light microscope work. Boothroyd noted that cell membranes were "scarcely visible" whereas they were quite clear in osmium postfixied tissue in this study (although invisible in glutaraldehyde only fixed tissue). The addition of osmium greatly enhanced Boothroyd's high temperature ash patterns (such as those from mitochondria) whereas osmium enhanced only a few, fine details in this study. This similarity between the glutaraldehyde and osmium fixed ash patterns was more striking than the differences. Low temperature ashing seemed to yield more organized detail, richer ash patterns, and perhaps more three-dimensional information than did high temperature ashing. These opinions cannot be conclusive until high and low temperature incineration is performed on the same tissues prepared in the same ways and sectioned at identical thicknesses.

The literature on electron microscopy (see Introduction) of the shell gland extensively describes the epithelial granules shown in Figs. 1 and 2. This paper has provided insight into the nature of these granules. Because a very dense ash remains, the granules cannot be entirely organic. However, the way the granules contract and shrink during ashing suggests that they are not pure mineral. It is likely that they are organic-metallic complexes, mineral bound within an organic framework that collapses into a dense ball when the organic support is removed. This factor is significant because all proposed roles for the granules have been for the production of organic components of eggs such as proteins or mucopolysaccharides for forming shell matrix, cuticle, or mammillary layer matrix (Richardson, 1935; Johnston et al., 1963; Breen and De Bruyn, 1969). The questions involved in the function of the shell gland cells are even more

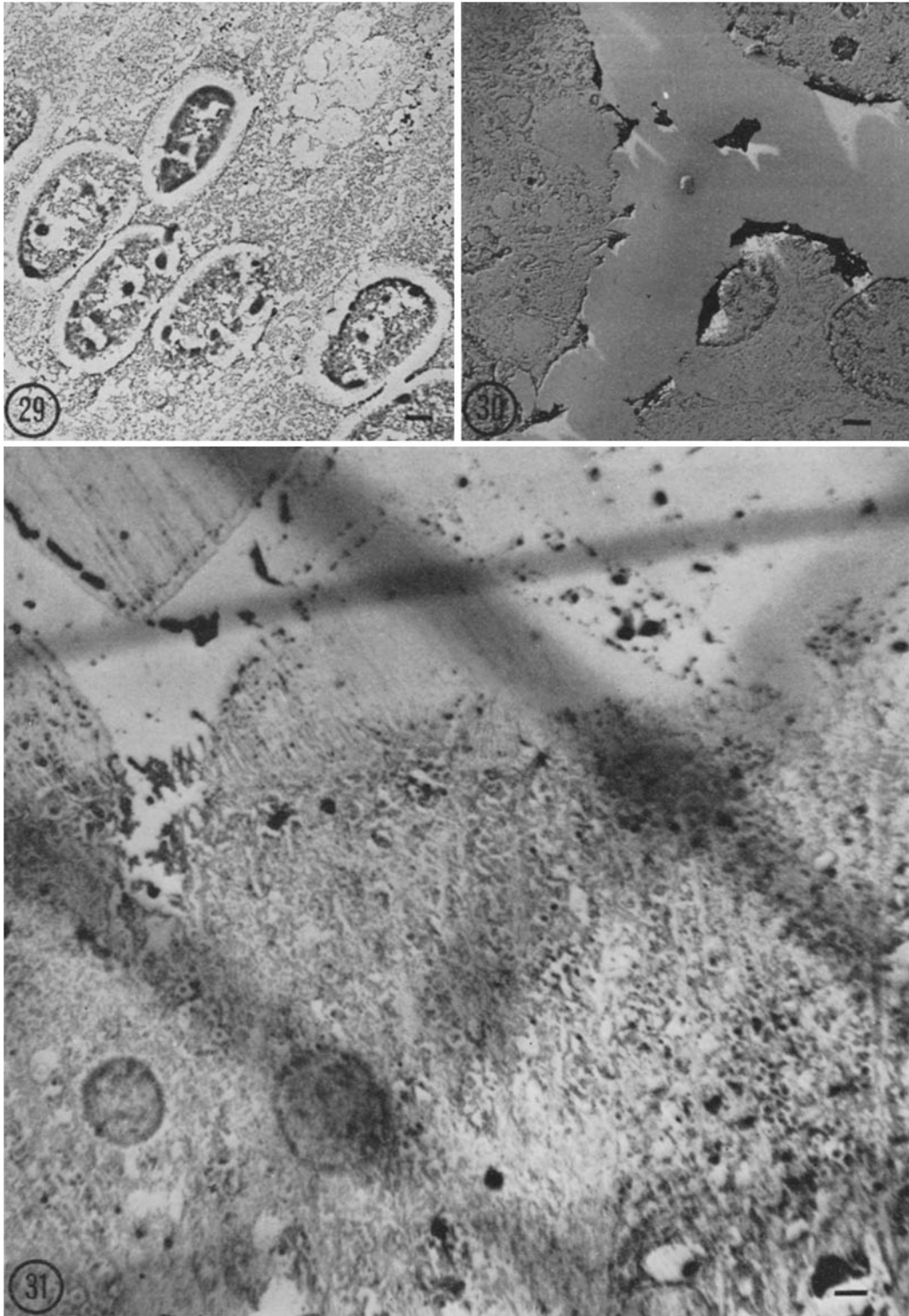
broad than indicated by the confusion on the roles of the granules. The basic question of whether the epithelial or gland cells have the major responsibility for the calcium transport has eluded investigators for many years (Cushny, 1902; Surface, 1912; Giersberg, 1922; Turchini, 1924; McCallion, 1953; Johnston et al., 1963; Hohman, 1967; Breen and De Bruyn, 1969; Gay and Schraer, 1971). Hohman (1967) and Schraer and Schraer (1970) have reviewed the history of this problem. In spite of the large quantities of calcium transported, the shell gland does not store large quantities of calcium and, therefore, concentrations are low and transient (Schraer and Schraer, 1965, 1971). However, it is not the purpose of this investigation to either solve the calcium secretion problem or to debate the role of the granules. This work only indicates that the large numbers of epithelial granules in the epithelial lining cells could be more involved in mineral transport than previously credited, and any future satisfactory elucidation of the granules' roles must consider their significant ash content. In contrast to the epithelial cells, the ashed gland cells do not contain specific, dense, ash concentrations.

The ultimate goal of metal/mineral localization in cells is to identify the ash elements *in situ* at the electron microscope level. Although a few exploratory steps were attempted in this direction, the only recourse at this time is to discuss the presumed mineral content of the shell gland. The mineral content of the whole shell gland tissue has been measured by Schraer and Schraer (1965). Without regard for the physiological state of the tissue, the mean quantity of ash remaining after treatment at 555° C for 5 hr was 65.1 ± 1.5 mg/g dry weight or about 6.5% of the total dry weight. This ash contained approximately 22.5% K, 13.0% Na, 2.4% Ca, 2.0% Mg, 0.5% Fe, 0.1% Zn, 0.01% Cu, and 0.009% Mn on a per cent ash basis. P was also

FIGURE 29 Ash residue from a 2.0 μ section of epithelial cells (glutaraldehyde fixed). The distortion at this thickness is especially evident by the wide clear zones around the nuclei. $\times 4000$.

FIGURE 30 An extreme example of ash distortion. This occurs when a fold in the section is ashed and there is no contact between the section and its support film (glutaraldehyde fixed, osmium postfixied, platinum shadowed). $\times 4000$.

FIGURE 31 Electron micrograph showing the tracks produced by the focused electron beam of the electron microprobe. The specimen was glutaraldehyde fixed, osmium postfixied, sectioned at 0.5 μ , low temperature ashed, scanned in the electron microprobe, and then photographed in the electron microscope. $\times 5000$.



likely to be present in significant quantities but it was not measured in this study. If the tissue could be prepared for electron microscopy without disturbing the arrangement of minerals, at least those metals listed would be present somewhere in the tissue. However, the tissue processing procedures which led to the final spodograms undoubtedly influenced the patterns and abundancies of these metals. Care was exercised to avoid adding exogenous elements during processing, but preventing the loss of endogenous elements was difficult. There are two factors that can alter the ash distribution and retention: aqueous solutions and the low temperature ashing.

The tissue is exposed to aqueous solutions during fixation and preparation for embedding as well as during sectioning. Preliminary, non-quantitative experiments with the fixing and embedding of Ca-45 labeled shell gland and rat liver mitochondrial pellets showed that a significant quantity of the radioisotope was lost in the aqueous fixatives and dilute alcohols from both glutaraldehyde and osmium fixed material. Renaud (1959) noticed this same problem, some loss of Ca in aqueous formalin fixative but minimal loss in 80% alcoholic-formalin. Other studies (Boothroyd, 1964, 1968; Thomas, 1964, 1969) have shown that Na and K and, in one case, Cu (Thomas, 1964) are lost during aqueous treatments. It is likely that these mineral losses occurred during shell gland preparation. Likewise, the minerals are very subject to loss and rearrangement during sectioning when the sections float on water. For this reason, Thomas (1969) used 0.001 M ammonium bicarbonate and Boothroyd (1964) used a saturated $\text{Ca}_3(\text{PO}_4)_2$ solution in the section trough to reduce mineral loss. Following Thomas's example, 0.001 ammonium bicarbonate was used in this study.

From this brief discussion, the most likely structure-bound elements surviving treatment are Ca, Mg, Fe, Zn, Mn, and P even though several of these (Ca, for example) may have been partially lost. Possible ways to avoid aqueous solutions are discussed by Boothroyd (1968) and Thomas (1969).

A second potential cause of mineral loss is the low temperature ashing procedure. However, studies have shown that most metals are retained during ashing. For example, 100% of the radioisotopes of Ca, Na, Mn, Fe, and Zn were retained as chloride salts in whole blood when low temperature ashed at a maximum temperature of less than 100° C (Gleit and Holland, 1962). Ca,

Mg, K, and Na were retained quantitatively (98.2–99.0%) from rat liver microsomes when ashed at 100–115° C (H. Sanui cited in Hollahan, 1966). Ca, Mg, Fe, Cu, and Zn from five bovine tissues low temperature ashed at 150° C in the LTA-600 showed good analytical agreement with the results obtained with platinum crucible high temperature ashing at 500° C (M. Nathans et al. cited in Hollahan 1966). Although P has not been included in these low temperature recovery studies, there is evidence that P probably is retained during low temperature ashing (Hald, 1946; Thomas and Greenawalt, 1968; Thomas, 1969). Note that all the elements listed as most likely to be structure bound in the shell gland (Ca, Mg, Fe, Zn, Mn, and P) are 100% retained (with the possible exception of P for which no values are available) during low temperature ashing. Even the soluble metals (Na, K, and Cu) are retained during low temperature ashing; however, significant losses and rearrangements of these metals may have occurred before exposure of the specimen to the excited oxygen. Most of the retention studies referenced did not employ aqueous solutions. The retention of Na and K is important because these metals are generally considered to be volatile during conventional ashing at 550–600° C (Addink, 1951; Na and K references in Kruszynski, 1963). In general, the recovery of elements after low temperature ashing (Gleit and Holland, 1962; Gleit, 1963; Hollahan, 1966) compared with high temperature ashing (Thiers, 1957; Gorsuch, 1959; Pijck et al., 1961) showed that the LTA always improved (sometimes considerably) or maintained the same elemental retention. Finally, the chemical form in which some elements exist sometimes determines their fate in the ashing process. For example, when I was low temperature ashed as NaI, only 30% was retained; however, 100% of NaIO_3 was retained (Gleit and Holland, 1962). Other examples have been cited in Hald (1933), Thiers (1957), Johnson (1960), Johnson and Pani (1962), Lillie (1965), and Hollahan (1966). These considerations could be especially important in low temperature ashing since the ashing process is chemical rather than thermal.

Two elements that do not occur normally in the shell gland were introduced for specific purposes in this study, lead and osmium. Lead, as $\text{Pb}(\text{NO}_3)_2$ in blood, was retained 100% in the LTA (Gleit and Holland, 1962), therefore, it probably remained in the ash shown in Figs. 23 and 24. The fate of osmium in the LTA is un-

clear. It might be expected that reduced osmium in the sample would reoxidize to OsO_4 during exposure to the excited oxygen and vaporize. Arnold and Sasse (1963) reported ash residues that were less than expected if osmium was retained. Thomas and Greenawalt (1968) found relatively little difference between osmium fixed and aldehyde fixed mitochondria after low temperature ashing. Extensive comparisons of osmium fixed versus glutaraldehyde fixed tissue sections in this study revealed few differences in very fine details. In contrast to these results, Boothroyd's (1968) high temperature ash patterns yielded much more ash from osmium fixed cells. The fate of osmium during low temperature ashing remains unsettled (refer to Thomas, 1969, for a more detailed discussion of this problem).

As mentioned in the Experimental Results, a preliminary attempt was made in this study to specifically localize elements in cells with an electron microprobe. Ca and P were identified as being present in the ash which experimentally confirms the speculation that these elements (among others) were likely to be present in the ash. Detecting Ca and P proved that these two elements were present in sufficient quantities in 0.5μ sections to be measured and that they survived all the preparative treatments including exposure to aqueous solutions. It was not possible to specify where the Ca and P were located within the cells because the spatial resolution of the microprobe was not sufficient. Galle (1967) used the electron microprobe to study thin sections (less than 0.1μ) of pathological kidney tissue and Thomas (1969) successfully identified P in sectioned, ashed virus preparations. Improved instrumentation for X-ray microanalysis could lead to *in situ* identification of metals and/or mineral within cells in the future. The future potential of intracellular mineral localization is much more optimistic today than it was in 1935 when Richardson wrote: "To take an individual cell and to define the exact regions of the cytoplasm where certain inorganic elements are located after incineration is not to be expected."

Because this work was exploratory in nature, a few of the technical problems warrant discussion. For example, considerable difficulty was experienced by the authors in developing a routine method for successfully preparing smooth, flat SiO support films. Simple vacuum evaporation of SiO onto Formvar-coated molybdenum grids resulted in wrinkled and unstable surfaces. The

final technique which evolved during this study yielded stable support films with minimal (but not eliminated) wrinkling. Thomas (1969) and Boothroyd (1968) also discuss the difficulties in preparing flat, SiO support films.

Another technical problem of any incineration study is the temperature of ashing. Attempts to measure the temperature directly on the grids during ashing (within the sealed LTA chambers) with a noncontact, infrared pyrometer were unsuccessful. In lieu of direct measurements, other studies may provide a reasonable estimate. Data from Tracerlab Div. showed that human blood serum ashed at only 175°C when the power level (300 watts) of the LTA was six times greater than that used in this study (50 watts). A sample protein (albumin) and two amino acids (unspecified) ashed well below 100°C even though power levels in both cases were approximately two times greater than the 50 watts used in this study. It should be noted that the ashing temperature is not a simple function of the power input. The temperature is influenced by the rate of reaction which is dependent upon exposed surface area (rather than mass), formation of ash crusts (which effectively reduces surface area), concentration of excited oxygen (which is dependent on flow rate, pressure, and radio frequency power input), and the chemical nature of the sample (Gleit and Holland, 1962; Bersin, 1965). Since low power levels, thin sections with large exposed surface areas, and predominantly organic samples were used in this study, it is estimated that the temperature on the electron microscope grids was less than 100°C in comparison with the cited measurements. This contrasts with the $500\text{--}600^\circ \text{C}$ temperatures used in high temperature ashing.

It was shown in the Experimental Results, with such examples as cell membranes (Figs. 13, 16, 23), mitochondria (Fig. 15), and collagen (Fig. 22), that good resolution could be obtained when thin sections were low temperature ashed. However, as section thickness increased, resolution became poorer in spite of the relatively gentle incineration methods of low temperature ashing which avoided the burning, melting, charring, etc. which are characteristic of high temperature ashing. The critical factor that seemed to be the ultimate source of resolution loss during low temperature ashing was the distance between the bulk of a sample and its support film. Apparently the inorganic residues collapsed upon the support films as the excited oxygen removed and

destroyed the supporting organic framework, a process that permitted migration of the ash. In very thin sections the inorganic material settled near its original locus and ash migration was minimal. In thicker sections, the ash seemed to migrate laterally as its vertical "collapse distance" increased. The lower limit of resolution occurred when the quantity of ash was too small to be observed. Figs. 13 and 23, for example, were near this limit. The upper limit of resolution occurred when the ash patterns became too distorted to permit recognition of the structures of specific interest. In this study, the intermediate section thickness of 0.5 μ was used commonly as a compromise between the visualization problems of thin sections (about 0.1 μ) and the ash distortion in thick sections (1 μ or more). Recognizing the causes of resolution loss can sometimes be useful because distortions arise from the way a sample ashes, and this provides clues on both the organic and inorganic composition of the sample.

This study and the others referenced (see Thomas' review, 1969) have demonstrated the current capabilities of low temperature incineration. It is clear that this technique may be used for many applications at its present level of development. If several technical advances develop, the information gained from low temperature ashing would increase many fold. One of these technical advances could be to improve mineral retention. One excellent method to avoid aqueous solutions is to section frozen material. Since ultrathin cryosectioning is becoming more advanced, this technique could be used with low temperature ashing in the future. Low temperature ashing of frozen sections would enhance the ash patterns since the main problem with aqueous solutions is mineral loss. Another technical advance would be improved resolution capability (smaller spot size) of the electron microprobe (or the newer scanning electron microscope/microprobe combinations). Such an improvement would convert low temperature ashing from a qualitative tool to a quantitative tool. The identities and locations of minerals within cells would then be possible. Finally, many more pathways may be explored by expanding the current technique. For example, careful mapping before ashing could facilitate studies with thin sections. Various histochemical methods could be used on the ash to aid in characterizing its composition. Density measurements could provide information on the mass of the ash. Classically, microincineration techniques have been

considered useful only as a gross morphological tool. This study has shown that the refined methods of low temperature ultramicroincineration may be used as a histological tool for the study of many biological materials.

The authors wish to acknowledge Dr. Rosemary Schraer for her counsel in many phases of this work, Dr. Eugene White and Mr. William Zeigler of the Materials Research Laboratory for providing the electron microprobe facilities, and Mrs. Bridget Stemberger and Mr. Carl Harpster for their technical assistance.

The research was supported, in part, by a National Institute of Dental Research grant (No. DE 01764). The first author was supported by a National Institute of General Medical Sciences Fellowship for the duration of the research project.

Received for publication 20 September 1971, and in revised form 19 June 1972.

REFERENCES

- ADDINK, N. W. H. 1951. Quantitative spectrochemical analysis by means of the direct current carbon arc. II. Biological Materials. A possible correlation between the zinc content of the liver and blood and the cancer problem. *Recl. Trav. Chim.* **70**:115.
- ARNOLD, M., and D. SASSE. 1963. Das Aschebild in elektronen Mikroskop. *Acta Histochem.* **3**(Suppl.): 204.
- BENNETT, H. S., and J. H. LUFT. 1959. S-collidine as a basis for buffering fixatives. *J. Biophys. Biochem. Cytol.* **6**:113.
- BERSIN, R. 1965. LTA-600 low temperature dry asher, technical applications guide. Tracerlab, Inc., Richmond, California.
- BOOTHROYD, B. 1964. The problem of demineralization in thin sections of fully calcified bone. *J. Cell Biol.* **20**:105.
- BOOTHROYD, B. 1968. The adaptation of the technique of micro-incineration to electron microscopy. *J. R. Microsc. Soc.* **88**:529.
- BRADLEY, D. E. 1965. Replica and shadowing techniques. In *Techniques for Electron Microscopy*. D. H. Kay, editor, F. A. Davis Company, Philadelphia, 2nd edition. 140.
- BRADLEY, O. C. 1928. Notes on the histology of the oviduct of the domestic hen. *J. Anat.* **62**:339.
- BREEN, P. C. 1966. The fine structure of the secretory cells of the uterus (shell gland) of the chicken. *Anat. Rec.* **154**:321. (Abstr.)
- BREEN, P. C., and P. P. H. DE BRUYN. 1969. The fine structure of the secretory cells of the uterus (shell gland) of the chicken. *J. Morphol.* **128**:35.
- CUSHNY, A. R. 1902. On the glands of the oviduct in the fowl. *Am. J. Physiol.* **6**:XVIII.

- DOBERENZ, A. R., and R. W. G. WYCKOFF. 1967. The Microstructure of Fossil Teeth. *J. Ultrastruct. Res.* **18**:166.
- DRUMMOND, D. G. 1950. The practice of electron microscopy. *J. R. Microsc. Soc.* **70**:1.
- ELIAS, L., E. A. OGRYZLO, and H. I. SCHIFF. 1959. The study of electrically discharged O₂ by means of an isothermal calorimetric detector. *Can. J. Chem.* **37**:1680.
- FONER, S. N., and R. L. HUDSON. 1956. Metastable oxygen molecules produced by electrical discharges. *J. Chem. Phys.* **25**:601.
- GALLE, P. 1967. Electron probe microanalysis of biological ultrathin sections. Second National Conference on Electron Microprobe Analysis, Boston, Mass. Abstract. 41.
- GAY, C. V., and H. SCHRAER. 1971. Autoradiographic localization of calcium in the mucosal cells of the avian oviduct. *Calif. Tissue Res.* **7**:201.
- GIERSBERG, H. 1922. Untersuchung über Physiologie und Histologie der Reptilien und Vögel; nebst einem Beitrag zur Fäsergeue. *Z. Wiss. Zool.* **120**:1.
- GLEIT, C. E. 1963. Electronic apparatus for ashing biologic specimens. *Am. J. Med. Electron.* **2**:112.
- GLEIT, C. E. 1965. High frequency electrodeless discharge system for ashing organic matter. *Anal. Chem.* **37**:314.
- GLEIT, C. E. 1966. Letter to the editor. *J. Chem. Educ.* **43**:392.
- GLEIT, C. E., and W. D. HOLLAND. 1962. Use of electrically excited oxygen for the low temperature decomposition of organic substances. *Anal. Chem.* **34**:1454.
- GLEIT, C. E., W. D. HOLLAND, and R. C. WRIGLEY. 1963. Reaction kinetics of the atomic oxygen-graphite system. *Nature (Lond.)*. **200**:69.
- GORSUCH, T. T. 1959. Radiochemical investigations on the recovery for analysis of trace elements in organic and biological materials. *Analyst. (Lond.)*. **84**:135.
- GREENAWALT, J. W., and E. CARAFOLI. 1966. Electron microscope studies on the active accumulation of Sr⁺⁺ by rat-liver mitochondria. *J. Cell Biol.* **29**:37.
- HALD, P. M. 1933. The determination of the bases of serum and whole blood. *J. Biol. Chem.* **103**:471.
- HALD, P. M. 1946. Notes on the determination and distribution of sodium and potassium in cells and serum of normal human blood. *J. Biol. Chem.* **163**:429.
- HASS, G., and H. T. MERYMAN. 1954. Silicon monoxide and its use in electron microscopy. Twelfth Annual Meeting of Electron Microscope Society of America, Highland Park, Illinois.
- HERRON, J. T., and H. I. SCHIFF. 1958. A mass spectrometric study of normal oxygen and oxygen subjected to electrical discharge. *Can. J. Chem.* **36**:1159.
- HOHMAN, W. 1967. A study of low temperature ultramicroincineration of the avian shell gland mucosa by electron microscopy. Ph.D. Dissertation. The Pennsylvania State University, University Park, Penna.
- HOHMAN, W., and H. SCHRAER. 1966. The intracellular distribution of calcium in the mucosa of the avian shell gland. *J. Cell Biol.* **30**:317.
- HOHMAN, W., and H. SCHRAER. 1967. Ultramicroincineration studies of the avian shell gland. *J. Cell Biol.* **35**(2, Pt.2):57A. (Abstr.)
- HOLLAHAN, J. R. 1966. XXVII. Analytical applications of electrodelessly discharged gases. *J. Chem. Educ.* **43**:A401.
- JOHNSON, B. 1960. Demonstration of sulfates of alkaline-earth metals in tissue sections. *J. Histochem. Cytochem.* **8**:332.
- JOHNSON, F. B., and K. PANI. 1962. Histochemical identification of calcium oxalate. *Arch. Pathol.* **74**:347.
- JOHNSTON, H. S., R. N. C. AITKEN, and G. M. WYBURN. 1963. The fine structure of the uterus of the domestic fowl. *J. Anat.* **97**:333.
- KAFIG, E. 1958. Preparation of large intact unsupported evaporated films. Research Report NM7101 00.07.01. Naval Medical Research Institute. Bethesda, Md. **16**:823.
- KAUFMAN, F., and J. R. KELSO. 1960. Catalytic effects in the dissociation of oxygen in microwave discharges. *J. Chem. Phys.* **32**:301.
- KORR, I. M. 1939. The osmotic function of the chicken kidney. *J. Cell. Comp. Physiol.* **13**:175.
- KRUZYNSKI, J. 1963. Bibliographia histochemica. Microincineration (spodographic) technique. *Acta Histochem.* **15**:58.
- LILLIE, R. D. 1965. Histopathologic Technic and Practical Histochemistry. McGraw-Hill Book Company, New York. 3rd edition. 652.
- LUFT, J. H. 1961. Improvements in epoxy resin embedding methods. *J. Biophys. Biochem. Cytol.* **9**:409.
- MAKITA, T., and S. NISHIDA. 1966. The fine structure of the avian oviduct. In Electron Microscopy. R. Uyeda, editor. Maruzen Co., Ltd., Tokyo, Japan. **II**:777.
- MARSH, H. T. E., O'HAIR, R. REED, and W. F. K. WYNNE-JONES. 1963. Reaction of atomic oxygen with carbon. *Nature (Lond.)*. **198**:1195.
- MARSH, H., T. E. O'HAIR, and W. F. K. WYNNE-JONES. 1965 a. Oxidation of carbons and graphites by atomic oxygen, kinetic studies. *Trans. Faraday Soc.* **61**:274.
- MARSH, H., T. E. O'HAIR, and R. REED. 1965 b. Oxidation of carbons and graphites by atomic oxygen, an electron microscope study of surface changes. *Trans. Faraday Soc.* **61**:285.
- MARTIN, J. H., and J. L. MATTHEWS. 1970. Mitochondrial granules in chondrocytes, osteoblasts, and

- osteocytes; an ultrastructural and microincineration study. *Clin. Orthop. Related Res.* **68**:273.
- MASER, M. D., T. E. POWELL III, and C. W. PHILPOTT. 1967. Relationships among pH, osmolality and concentration of fixative solutions. *Stain Technol.* **42**:175.
- MATTHEWS, J. L., J. H. MARTIN, H. W. SAMPSON, A. S. KUNIN, and J. H. ROAN. 1970. Mitochondrial granules in normal and rachitic rat epiphysis. *Calcif. Tissue Res.* **5**:91.
- MCCALLION, D. J. 1953. A cytological and cytochemical study of the shell gland of the domestic hen. *Can. J. Zool.* **31**:577.
- NEVALAINEN, T. J. 1969. Electron microscope observations on the shell gland mucosa of calcium deficient hens (*Gallus domesticus*). *Anat. Rec.* **164**:127.
- OGRYZLO, E. A., and H. I. SCHIFF. 1959. The reaction of oxygen atoms with NO. *Can. J. Chem.* **37**:1690.
- PIJCK, J., J. GILLIS, and J. HOSTE. 1961. La détermination du Cu, Cr, Zn, et Co dans le serum par radioactivation. *Int. J. Appl. Radiat. Isot.* **10**:149.
- RENAUD, S. 1959. Superiority of alcoholic over aqueous fixation in the histochemical detection of calcium. *Stain Technol.* **34**:267.
- RICHARDSON, K. C. 1935. The secretory phenomenon in the oviduct of the fowl, including the process of shell formation examined by the microincineration technique. *Philos. Trans. R. Soc. (Lond. Ser. B. Biol. Sci.)*. **225**:149.
- SABATINI, D. D., K. BENSCH, and R. J. BARNETT. 1963. Cytochemistry and electron microscopy. The preservation of cellular ultrastructure and enzymatic activity by aldehyde fixation. *J. Cell Biol.* **17**:19.
- SAMPSON, H. W., J. L. MATTHEWS, J. H. MARTIN, and A. S. KUNIN. 1970. An electron microscope localization of calcium in the small intestine of normal, rachitic, and vitamin-D-treated rats. *Calcif. Tissue Res.* **5**:305.
- SCHRAER, R., and H. SCHRAER. 1965. Changes in metal distribution of the avian oviduct during the ovulation cycle. *Proc. Soc. Exp. Biol. Med.* **119**:937.
- SCHRAER, R., and H. SCHRAER. 1970. The avian shell gland: A study in calcium translocation. In *Biological Calcification: Cellular and Molecular Aspects*. H. Schraer, editor. Appleton-Century-Crofts, New York. 347.
- SCHRAER, H., and R. SCHRAER. 1971. Calcium transfer across the avian shell gland. In *Cellular Mechanisms for Calcium Transfer and Homeostasis*. G. Nichols, Jr., editor. Academic Press Inc., New York. 567.
- SCOTT, G. H. 1933. The localization of mineral salts in cells of some mammalian tissues by microincineration. *Am. J. Anat.* **53**:243.
- SURFACE, F. M. 1912. Histology of the oviduct of the hen. *Maine Agric. Exp. Stn. Bull.* **206**:395.
- THIERS, R. E. 1957. Contamination in trace element analysis and its control. In *Methods of Biochemical Analysis*. V. D. Glick, editor. Interscience Publishers Inc., New York. 223.
- THOMAS, R. S. 1962. Demonstration of structure-bound mineral constituents in thin-sectioned bacterial spores by ultramicroincineration. In *Electron Microscopy*. S. S. Breese, editor. Academic Press Inc., New York. **2**:RR-11.
- THOMAS, R. S. 1964. Ultrastructural localization of mineral matter in bacterial spores by microincineration. *J. Cell Biol.* **23**:113.
- THOMAS, R. S. 1965. Ultrastructural localization of mineral constituents by microincineration and electron microscopy. *J. Cell Biol.* **27**(2, Pt.2):106A. (Abstr.)
- THOMAS, R. S. 1967. Microincineration and electron diffraction techniques for fine localization of biological mineral substances. *J. Ultrastruct. Res.* **21**:159.
- THOMAS, R. S. 1969. Microincineration for electron-microscopic localization of biological minerals. In *Advances in Optical and Electron Microscopy*. R. Barer and V. E. Cosslett, editors. Academic Press Inc., New York. **3**:99.
- THOMAS, R. S., and J. W. GREENAWALT. 1964. Microincineration of calcium phosphate-loaded mitochondria. *J. Appl. Physiol.* **35**:3083.
- THOMAS, R. S., and J. W. GREENAWALT. 1968. Microincineration, electron microscopy, and electron diffraction of calcium phosphate-loaded mitochondria. *J. Cell Biol.* **39**:55.
- TURCHINI, J. 1924. Sur l'histologie et l'histophysiologie de l'oviducte de la poule. *C. R. Assoc. Anat.* **19**:255.
- TURKEVICH, J. 1959. The world of fine particles. *Am. Sci.* **47**:97.
- VENABLE, J. H., and R. COGGESHALL. 1965. A simplified lead citrate stain for use in electron microscopy. *J. Cell Biol.* **25**:409.
- WILLIAMS, R. C. 1952. High resolution electron microscopy of the tobacco mosaic virus. *Biochim. Biophys. Acta.* **8**:227.